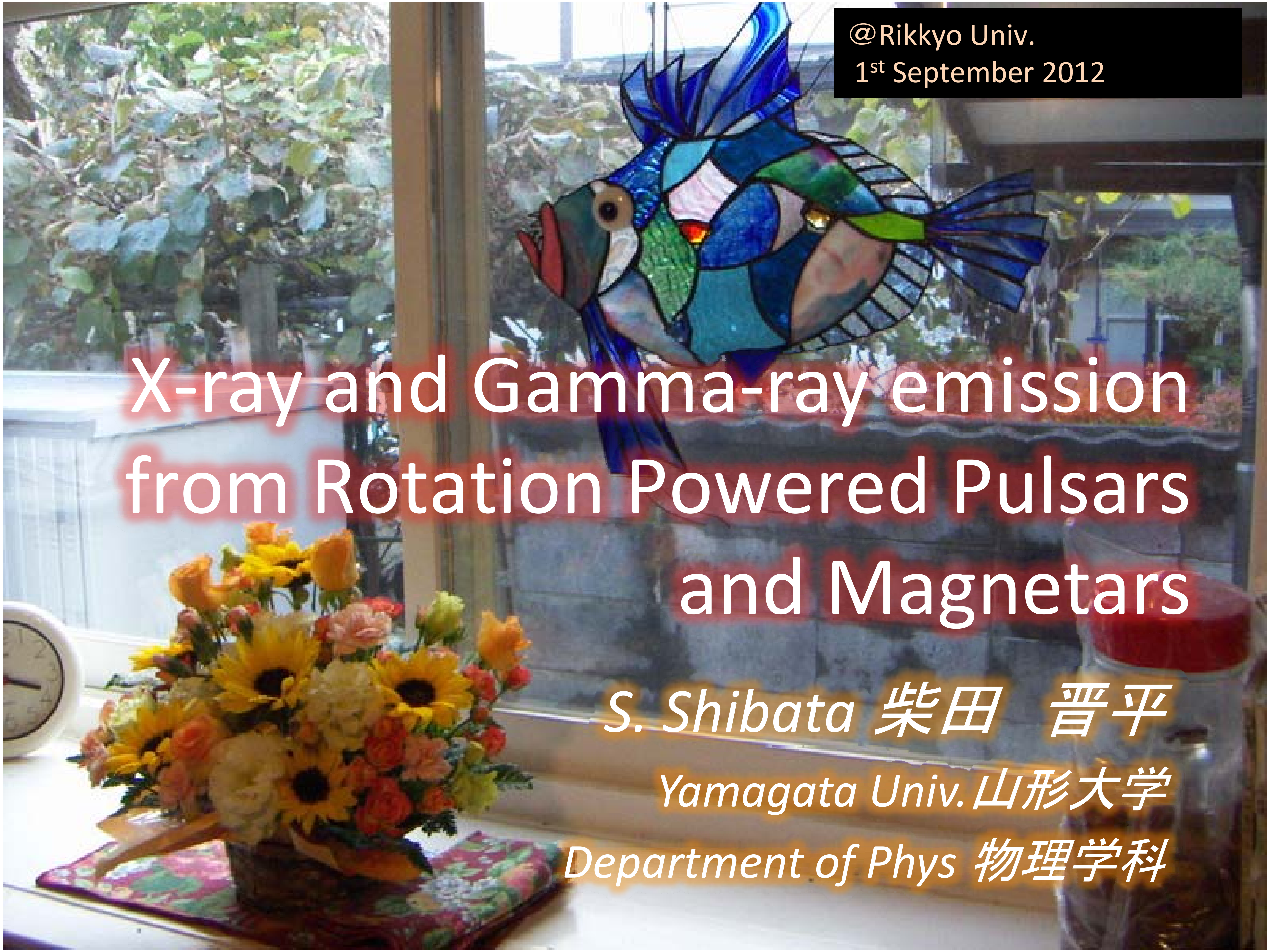

@Rikkyo Univ.
1st September 2012

X-ray and Gamma-ray emission from Rotation Powered Pulsars and Magnetars

S. Shibata 柴田　晋平
Yamagata Univ.山形大学
Department of Phys 物理学科

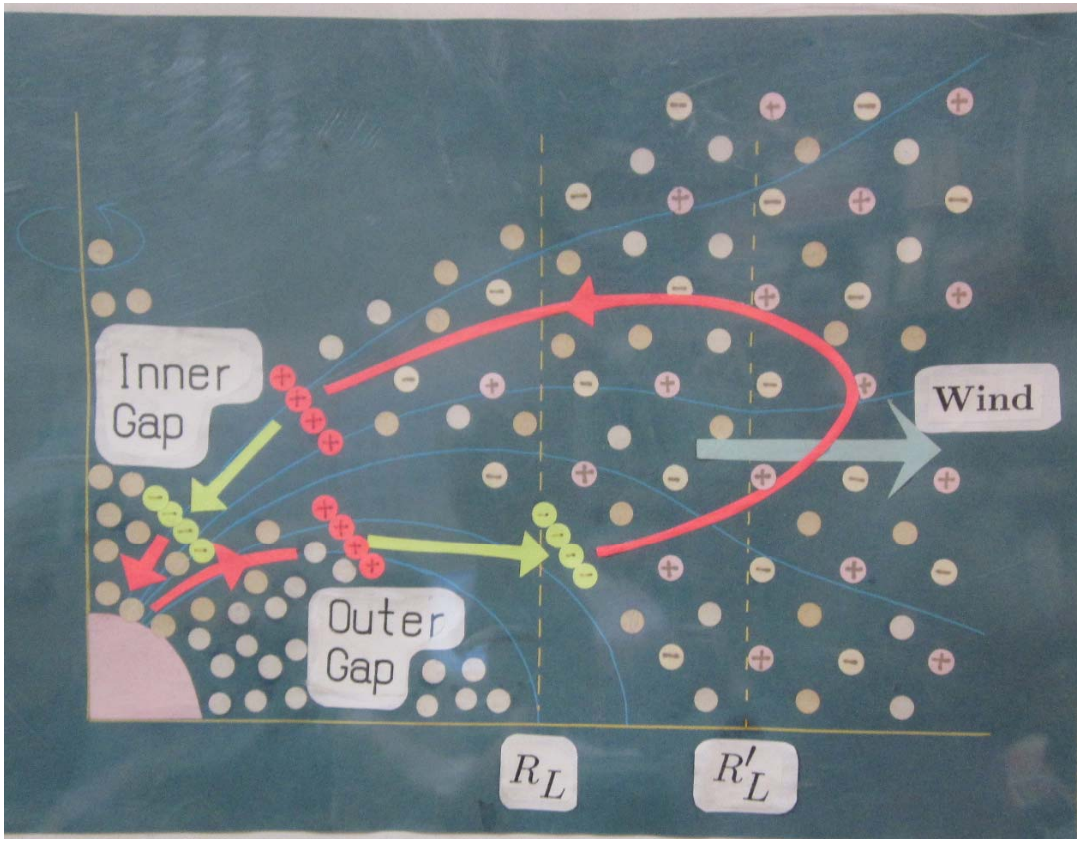

IAU Colloquium 128 in 1990, Pedagogical Univ.,Poland
the poster presented by Shibata S.
“A DC-Circuit Model of the Pulsar Magnetosphere”

outline

- study of the global structure of the aligned magnetosphere of RPP via particle simulation
- comparison with observations (Gamma-ray, X-ray,..., Radio)
- how magnetars are connected with RPP

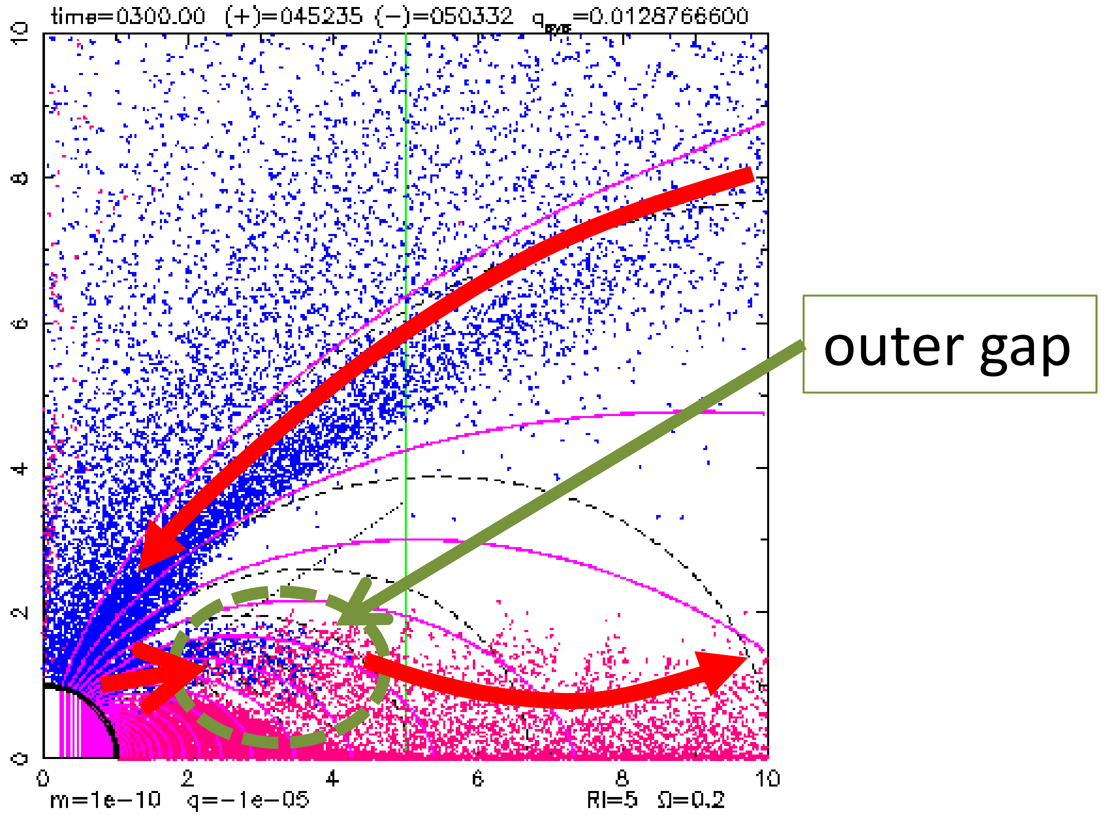

Yuki, S., Shibata, S., 2012, PASJ, 64, 43

Outer gap and the current system are reproduced in the simulation

outline

- study of the global structure of the aligned magnetosphere of RPP via particle simulation
- comparison with observations (Gamma-ray, X-ray,… Radio)
- how magnetars are connected with RPP

1. The outer gap can be reproduced under a few simple assumptions.

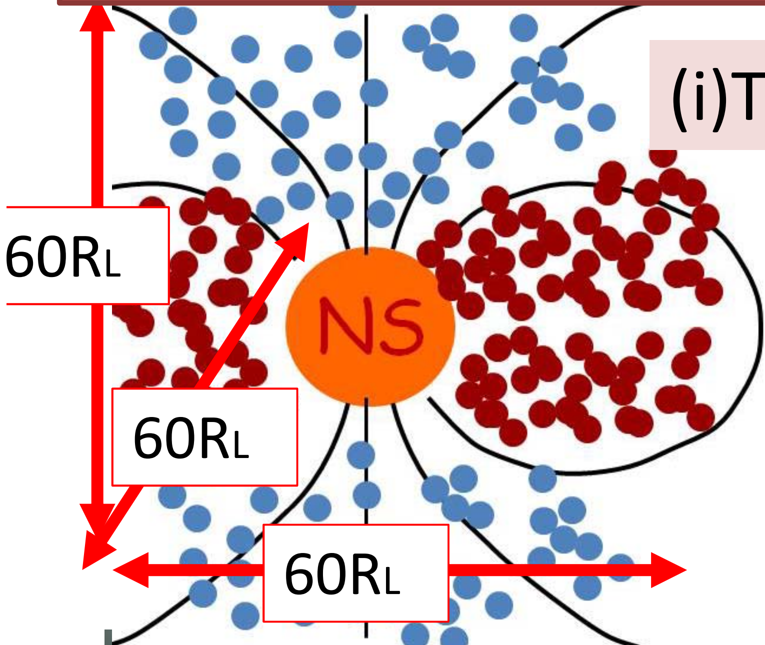

(i)The system is axis-symmetric,

$$-\nabla^2\phi = 4\pi\rho \quad \nabla\times\boldsymbol{B} = \frac{4\pi}{c}\boldsymbol{j}$$

Plasmas are represented by several tens of thousands of super-particles.

Cal .Domain is 3D (60RL)^3

GRAPE-6@nao.jp
Special purpose computer for
Astronomical N-body Problem

We iteratively solve the equation of mo. and EM field until steady state is settled down.

1. The outer gap can be reproduced under a few simple assumptions. (cont.)

(ii) rel. eq. mo. for super particles with radiation drag force.

$$\frac{\mathrm{d}\boldsymbol{p}_i}{\mathrm{d}t} = q_i \left[\boldsymbol{E}(\boldsymbol{r}_i) + \boldsymbol{\beta}_i \times \boldsymbol{B}(\boldsymbol{r}_i) \right] + \boldsymbol{F}_{\mathrm{drag},i}$$

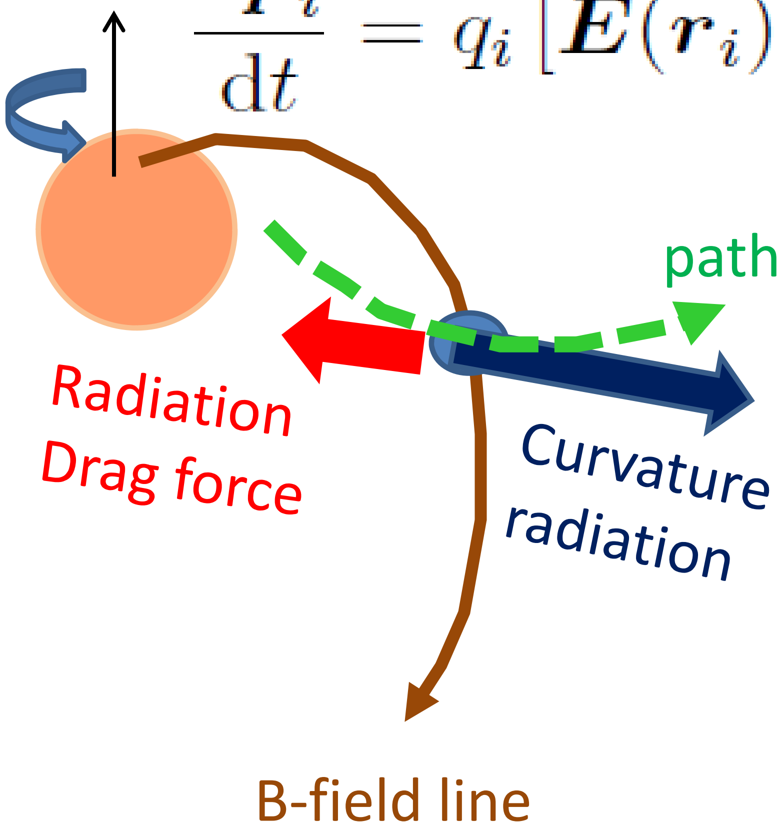

1. (m, q) are chosen so that any plasma drift motions are tracked correctly. dt<< gyro-period
2. Radiation drag force is taken into account in the lowest order approximation.

1. The outer gap can be reproduced under a few simple assumptions. (cont.)

(iii) Plasma sources are provided for
- free emission from NS surface
- pair creation if E// > Ec. (on the spot approx.)

model parameter

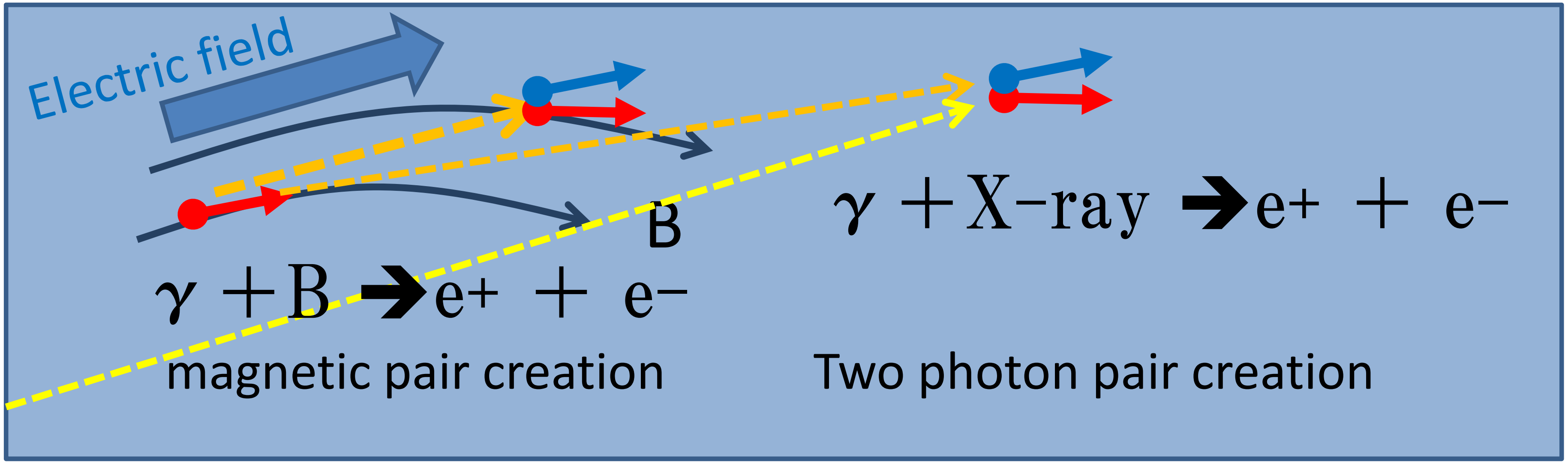

That's all!!!

1. The outer gap can be reproduced under a few simple assumptions. (cont.)

(*) Central magnet is rotating : i.e. voltage on NS

BC. on NS surface is strictly satisfied, because we use the Green function satisfying the boundary condition to obtain the electromagnetic field.

$$\phi = \phi_m + \phi_v$$

$$\boldsymbol{E} = \boldsymbol{E}_m + \boldsymbol{E}_v$$

$$\phi_m(\boldsymbol{r}) = \sum_{i=1}^{n} q_i \left[\frac{1}{|\boldsymbol{r} - \boldsymbol{r}_i|} - \frac{(R/r_i)}{|\boldsymbol{r} - (R/r_i)^2 \boldsymbol{r}_i|} - \frac{(1 - R/r_i)}{r} \right]$$

$$\boldsymbol{E}_m(\boldsymbol{r}) = \sum_{i=1}^{n} q_i \left[\frac{\boldsymbol{r} - \boldsymbol{r}_i}{|\boldsymbol{r} - \boldsymbol{r}_i|^3} - \frac{R}{r_i} \frac{\boldsymbol{r} - (R/r_i)^2 \boldsymbol{r}_i}{|\boldsymbol{r} - (R/r_i)^2 \boldsymbol{r}_i|^3} - \frac{(1 - R/r_i)\boldsymbol{r}}{r^3} \right]$$

$$\phi_v(\boldsymbol{r}) = -\frac{B_* \Omega R^2}{2c} \left(\frac{R}{r}\right)^3 \left(\cos^2\theta - \frac{1}{3}\right) + \frac{Q_t}{r}$$

$$\boldsymbol{E}_v(\boldsymbol{r}) = \left[-\frac{B_* \Omega R \, (3\cos^2\theta - 1)}{2c \, (r/R)^4} + \frac{Q_t}{r^2} \right] \boldsymbol{e}_{\mathrm{r}} - \left(\frac{\Omega B R \sin\theta \cos\theta}{c \, (r/R)^4} \right) \boldsymbol{e}_\theta$$

GRAPE-6@nao.jp
Special purpose computer for
Astrononomical N-body Problem

With this method, the corotation boundary (i.e. emf of the star) is strictly satisfied,

$$\phi(\boldsymbol{R}) = \frac{B_* \Omega R^2}{2c}\left(\sin^2\theta - \frac{2}{3}\right) + \frac{Q_t}{R} - \frac{Q_m}{R_m}$$

with

$$\phi(\infty) = 0$$

$$Q_m = \sum_{i=1}^{n} q_i$$

In general, surface charge on the star exists, but it is replaced by simulation particles (free emission) until no surface charge is emitted from the stellar surface.

$$\sigma = \sigma_m + \sigma_v$$

$$\sigma_m(\boldsymbol{R}) = \sum_i q_i \left\{ \frac{R^2 - r_i^2}{4\pi R} \frac{1}{|\boldsymbol{R} - \boldsymbol{r}_i|^3} - \frac{1}{4\pi R^2}\left(1 - \frac{R}{r_i}\right) \right\}$$

$$\sigma_v(\boldsymbol{R}) = \frac{B_* R^2 \Omega}{8\pi c}(3 - 5\cos^2\theta) + \frac{Q_t}{4\pi R^2}$$

For the magnetic field, we use

$$\boldsymbol{B}(\boldsymbol{r}) = \boldsymbol{B}_d + \sum_i \frac{q_i \boldsymbol{v}_i \times (\boldsymbol{r}_i - \boldsymbol{r})}{|\boldsymbol{r}_i - \boldsymbol{r}|^3}$$

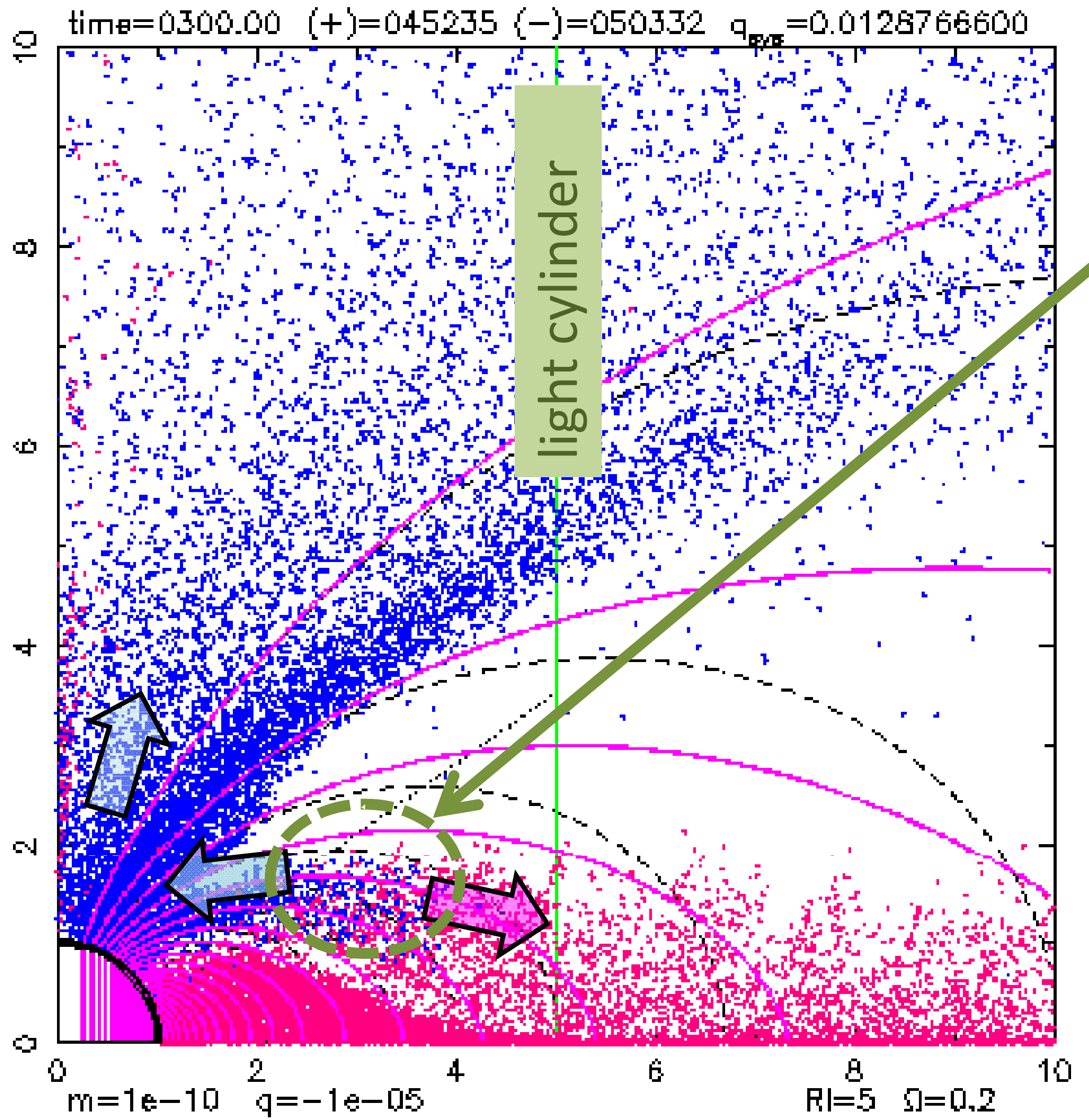

outer gap

Pairs are continuously produced.

Pairs are immediately separated by the field-aligned electric field.

E// map

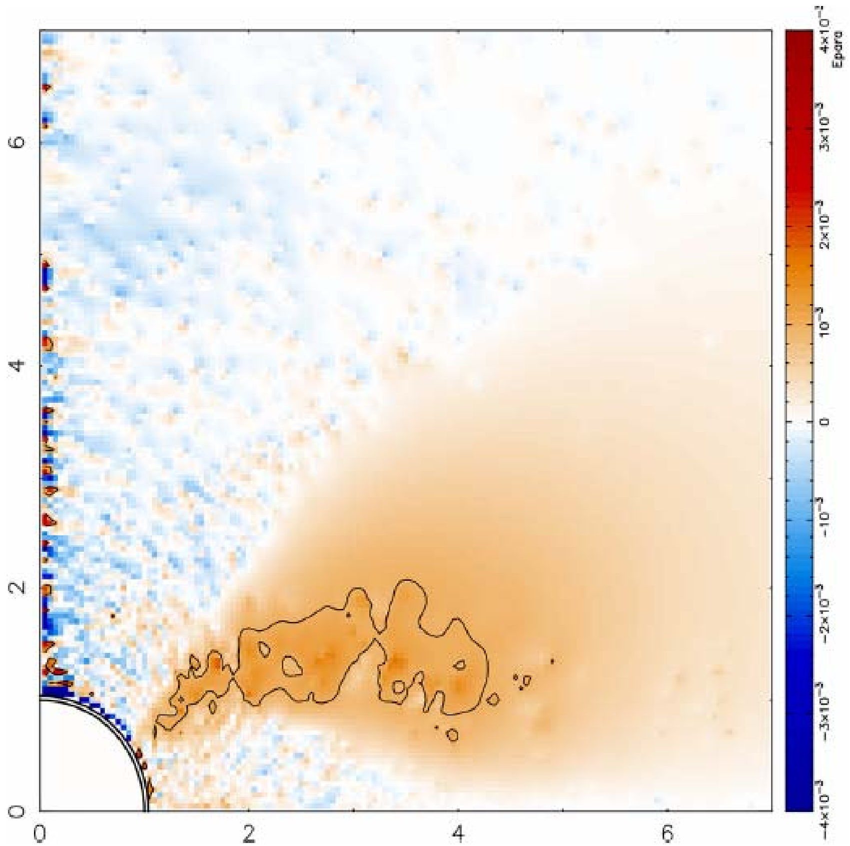

Because we have plasma sources, E// is screened out everywhere, except for the outer gap where E// is just above Ec: necessary minimum for pair creation.

2. Centrifugal driven particle acceleration at the top of the closed field region (Y-point). E-perp effect.

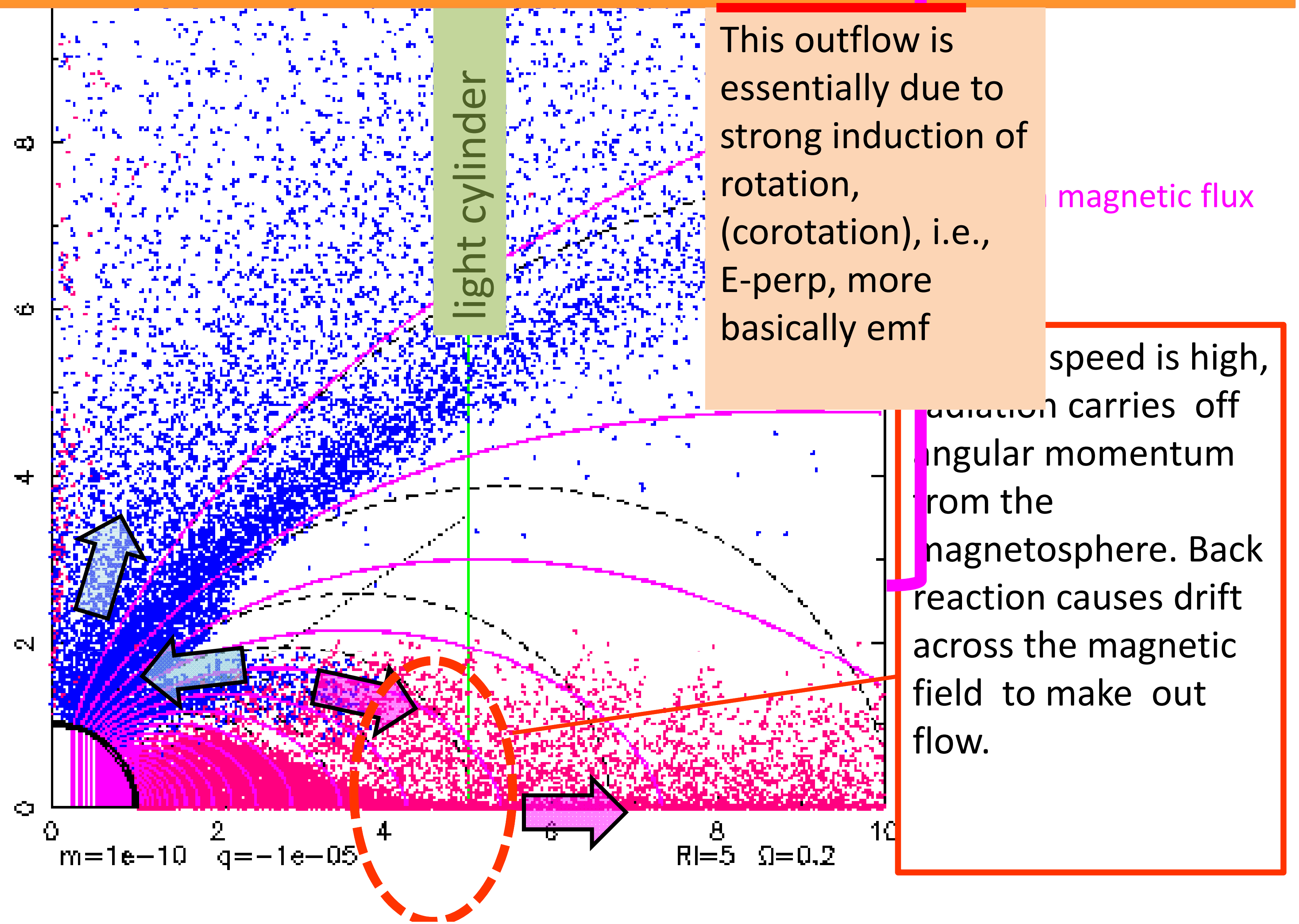

2. Centrifugal driven particle acceleration at the top of the closed field region (Y-point). E-perp effect. (cont.)

Force-free Udzdenski sol.

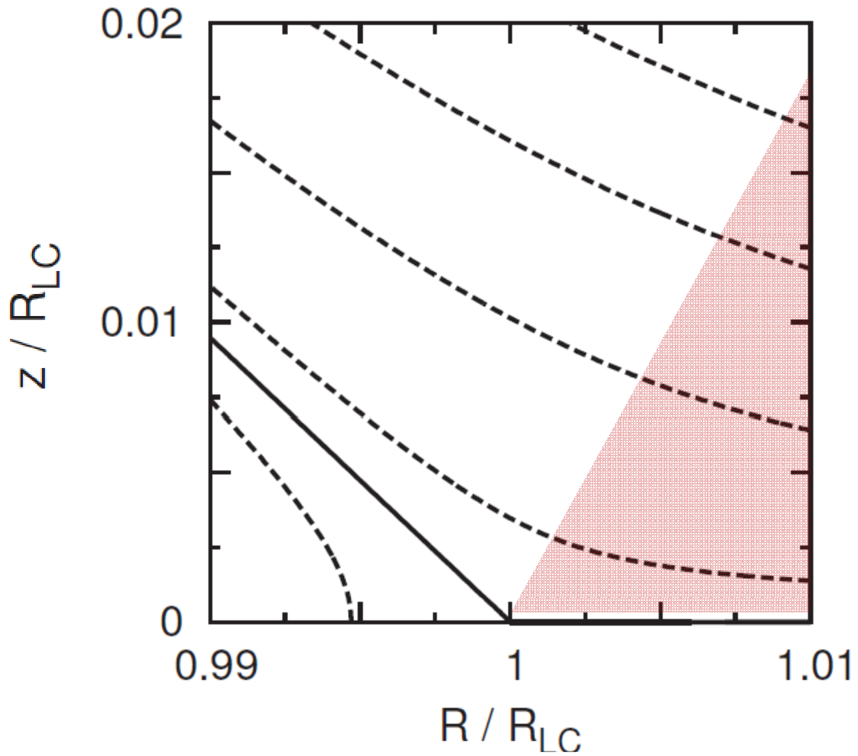

(Uzdensky, 2003)

Map of E/B

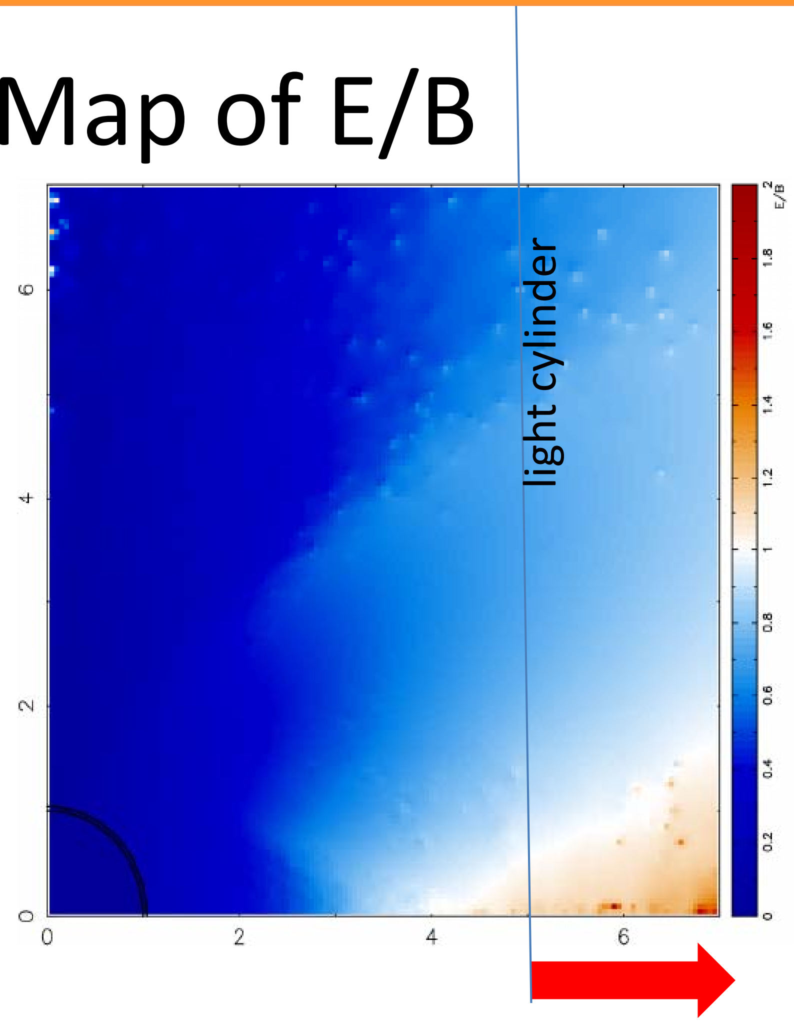

2. Centrifugal driven particle acceleration at the top of the closed field region (Y-point). E⊥ effect. (cont.)

centrifugal driven reconnection at the top of the closed field region

2-D cylindrical PIC simulation for Y-point.

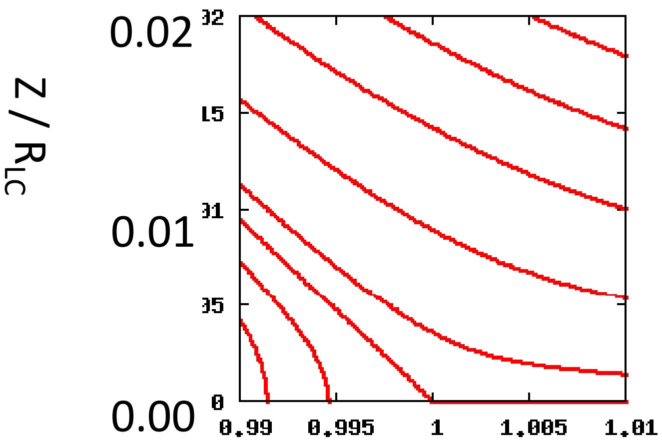

Initial state

(Uzdensky, 2003)

$t \sim 4 \times 10^5 \, \Delta t$

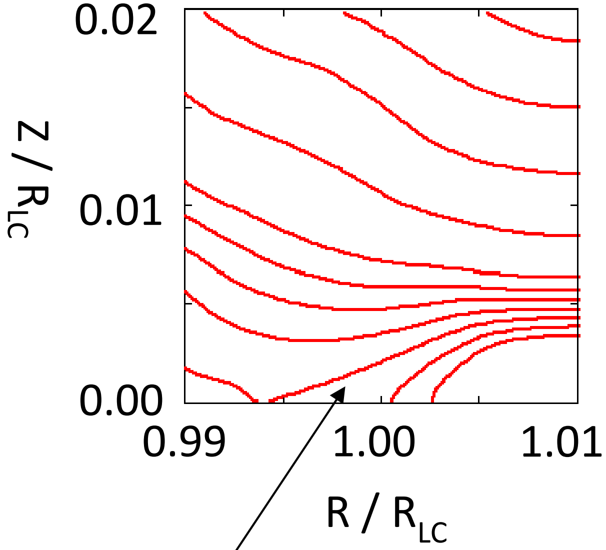

Magnetic reconnection takes place

⇒ heating and acceleretion

3. Dead zones along separatrix of the current is found. OG, PC locate above it and SG below it.

Map of Non-corotational electric potential

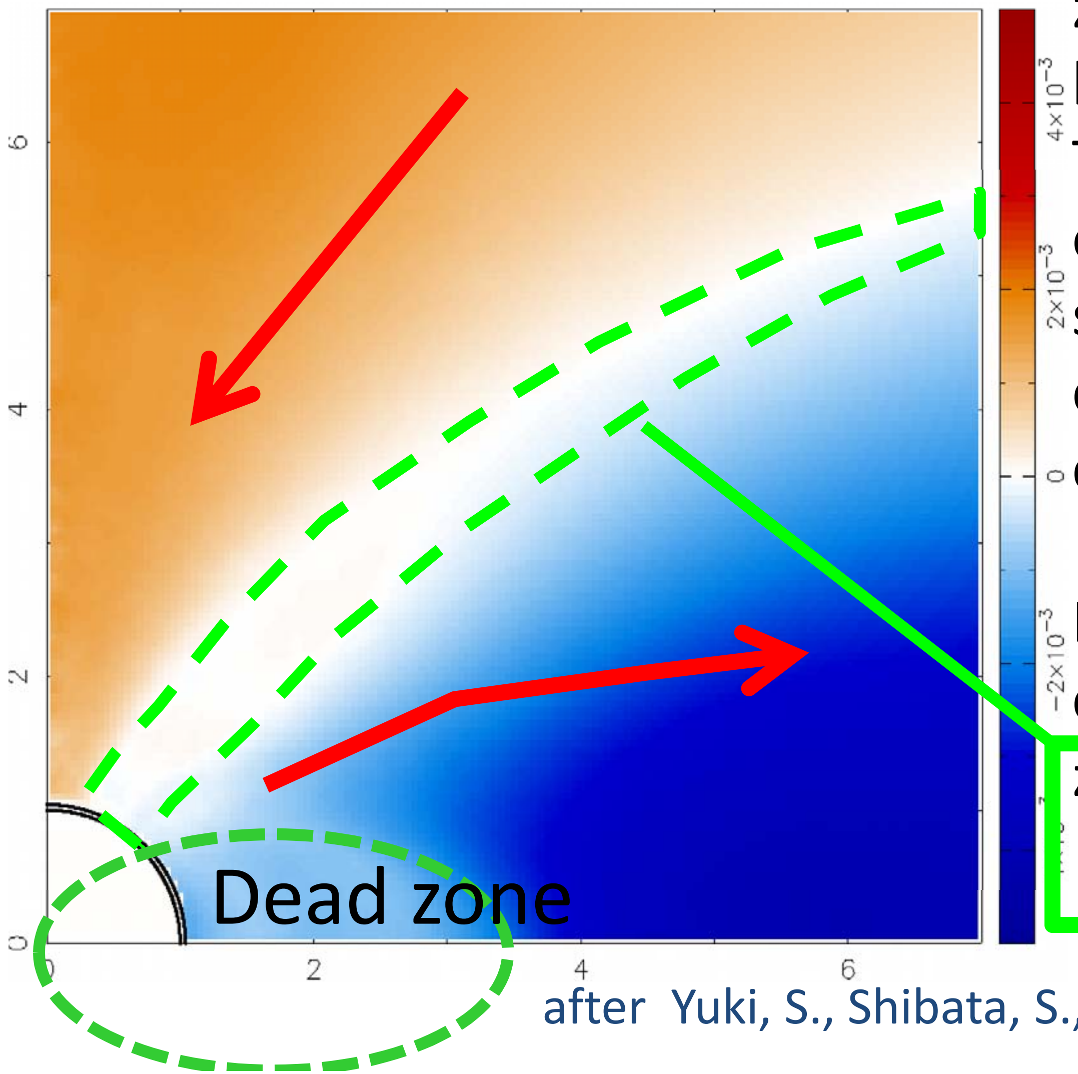

after Yuki, S., Shibata, S., 2012, PASJ, 64, 43

We find another dead zone in the middle latitudes.
This dead zone locates on the field lines which separates the outgoing current and ingoing current.

Let us call this zone the current neutral dead zone.

3. Dead zones along separatrix of the current is found. OG, PC locate above it and SG below it. (cont.)

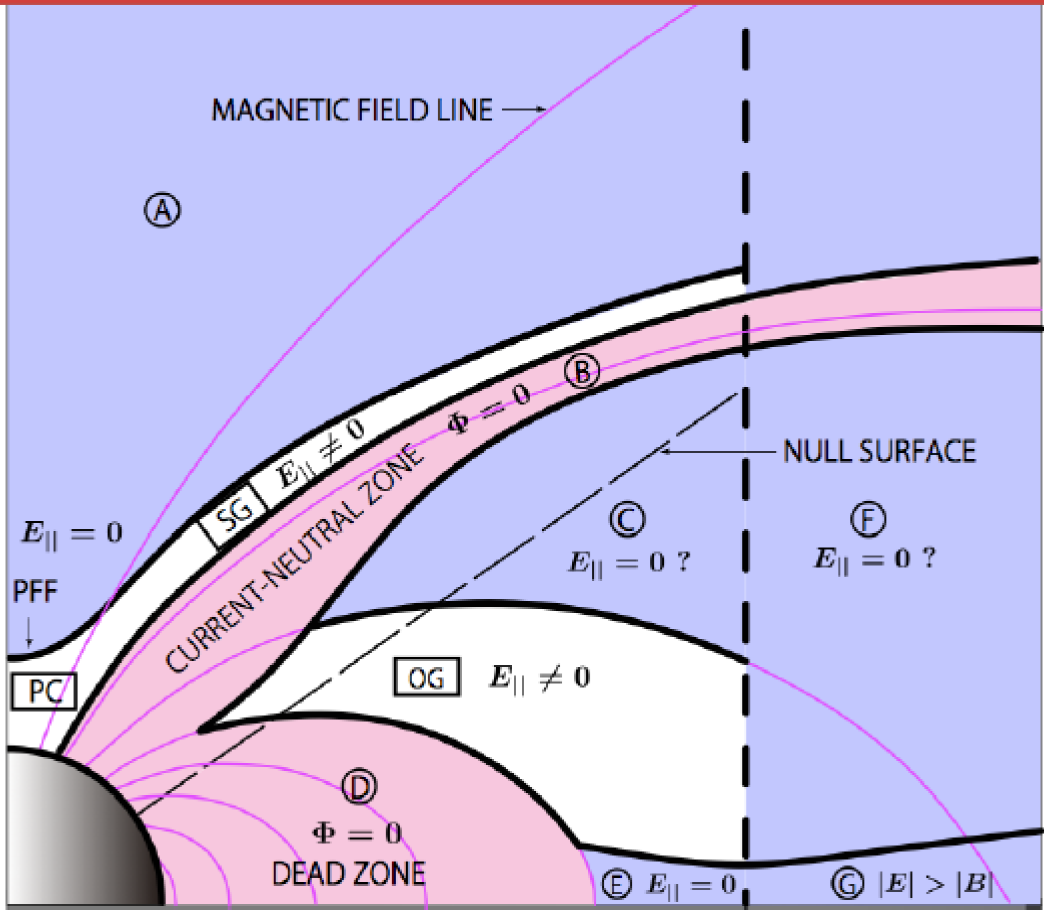

after Yuki, S., Shibata, S., 2012, PASJ, 64, 43

The outer gap is sandwiched by two dead zones. Therefore, the boundary conditions used previously in the outer gap is correct.

The polar cap and the slot gap would be above the current neutral dead zone.

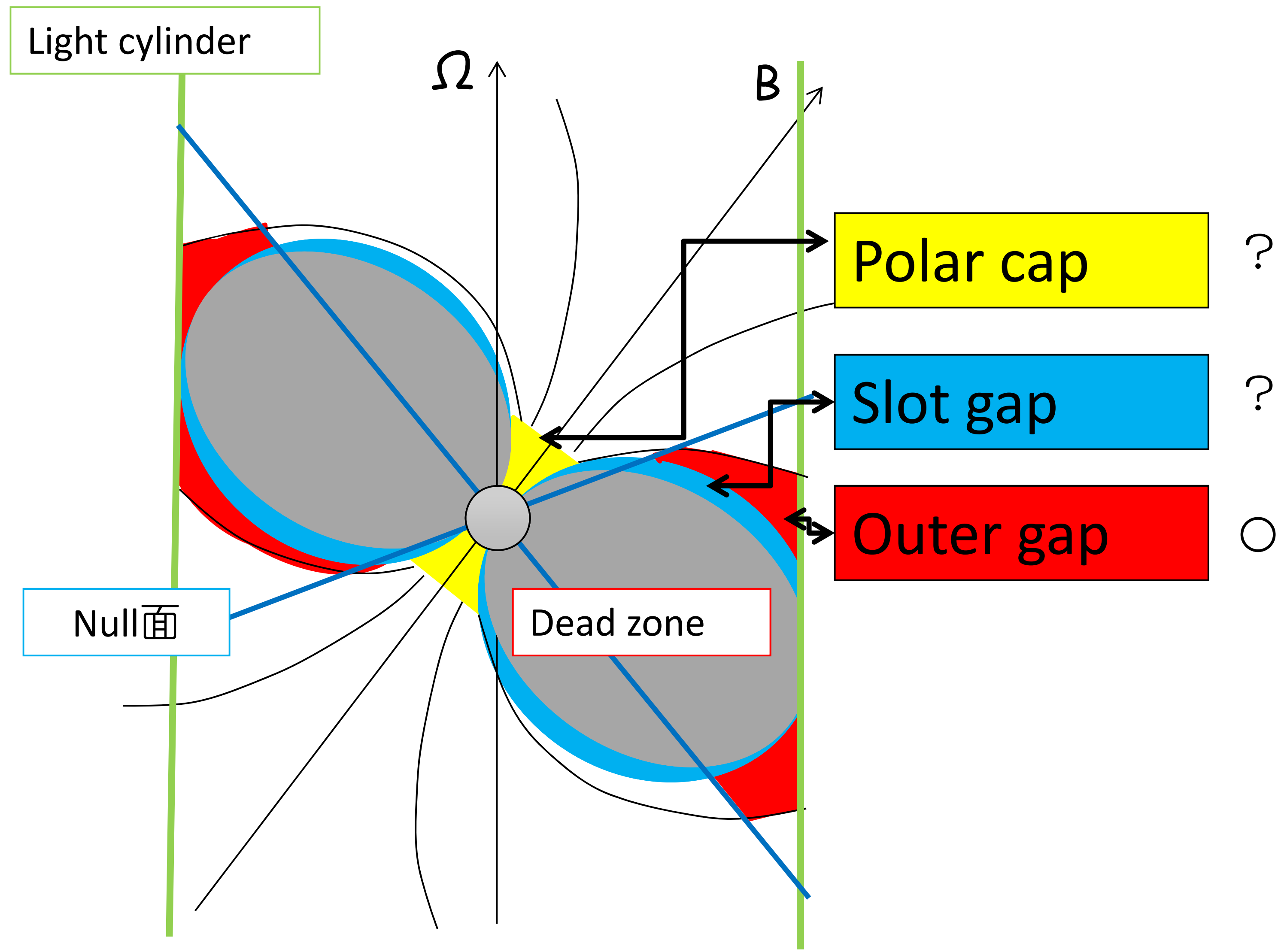

Light cylinder
Ω
B
Polar cap
?
Slot gap
?
Outer gap
○
Null面
Dead zone

comparison with observations (Gamma-ray, X-ray,… Radio)

Observation (Vela)

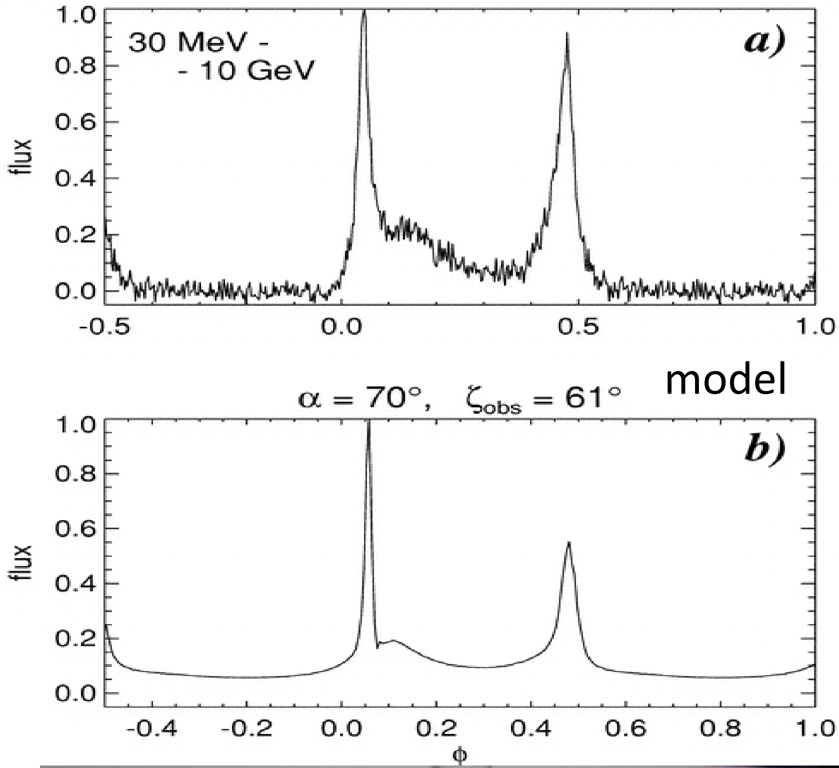

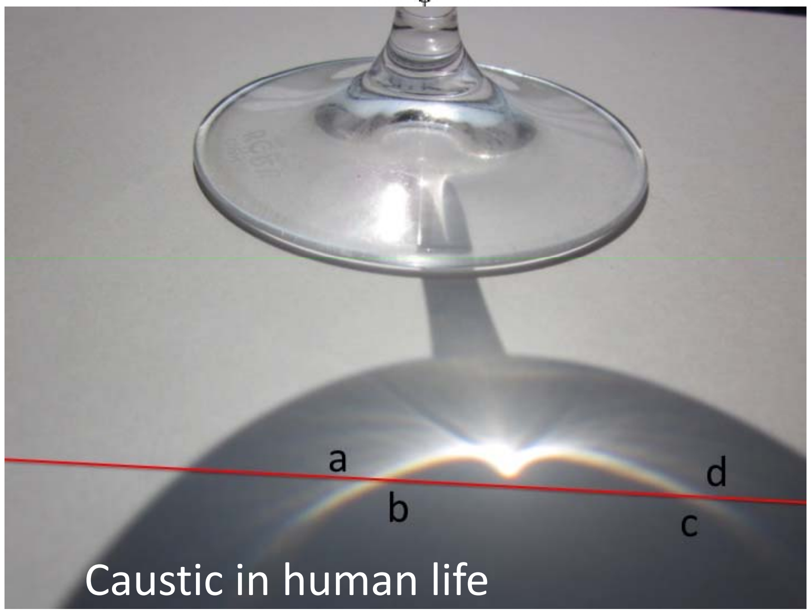

Double peak and bridge emission can be understood if emission is along the last open field lines; due to multi-ply superposition of photon arrival times: caustic.

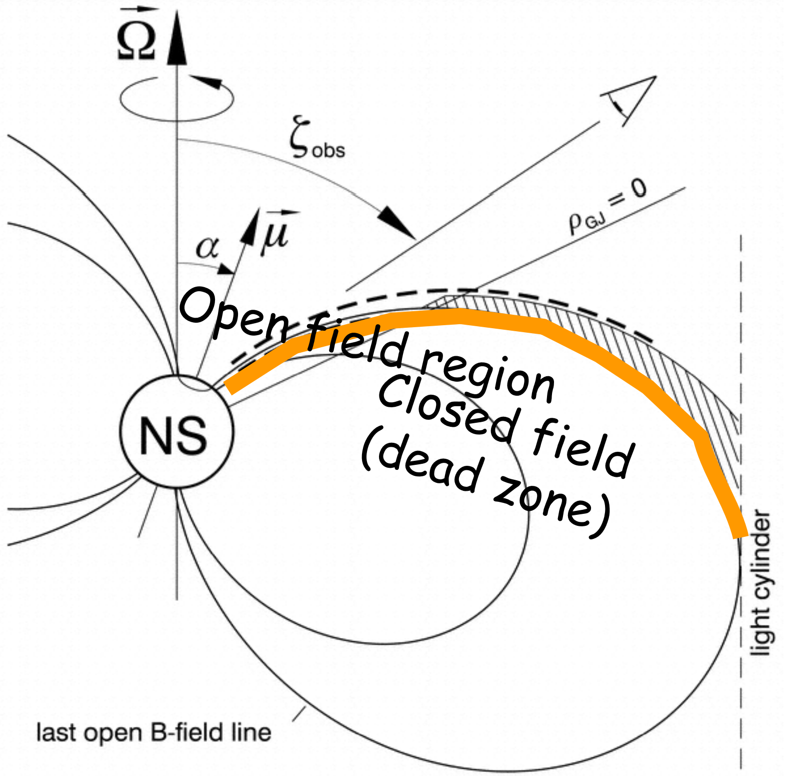

Two-pole caustic (TPC) geometry
(Dyks & Rudak, 2003)

Favors Slot gap / Outer gap

Outer gap modelの光度曲線

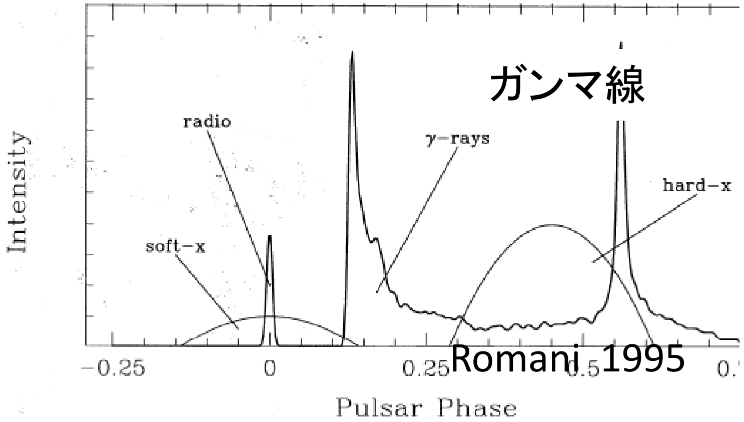

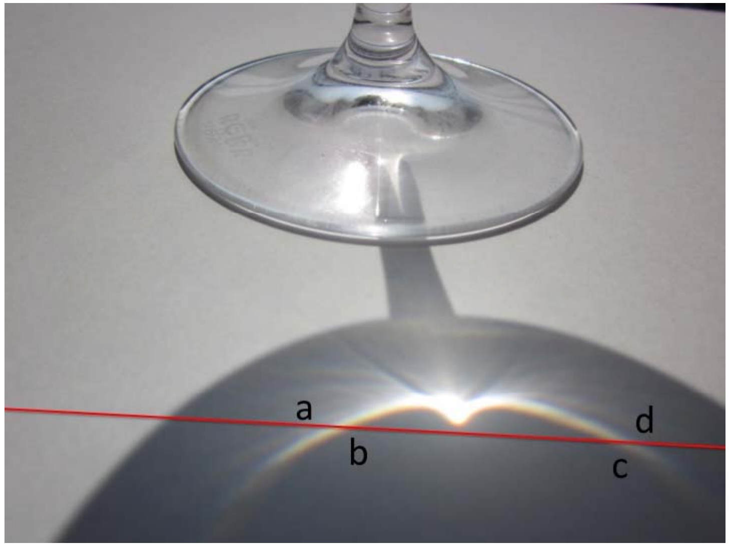

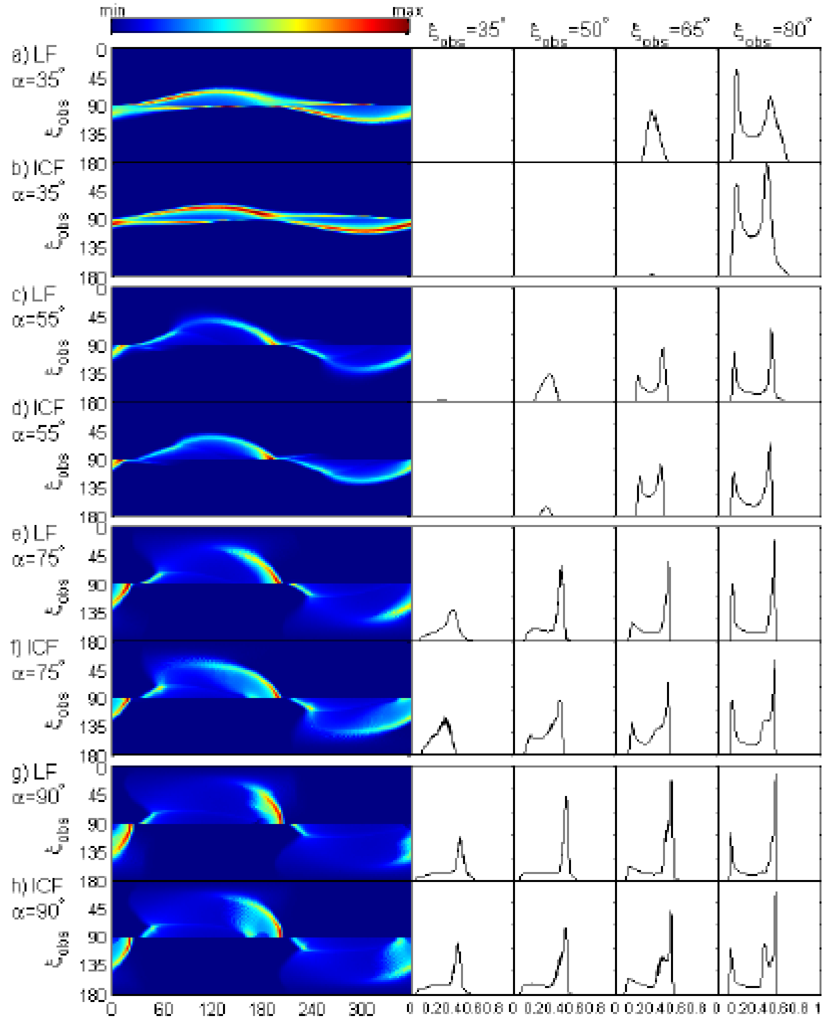

FIG. 7.— Atlas of sky maps and light curves for the outer gap (OG) model for representative pulsar inclination angles (constant for each row) and for different observer viewing angles (arranged in columns). Panels a), c), e), g) show results from treating the retarded field in the lab frame, while b), d), f), h) treat the field in the instantaneously corotating frame.

Bai & Spittkovskiy2009

FermiによるVela パルサーのガンマ線スペクトル

$$N(E) = N_0 E^{\Gamma} e^{-(E/E_c)^b}$$

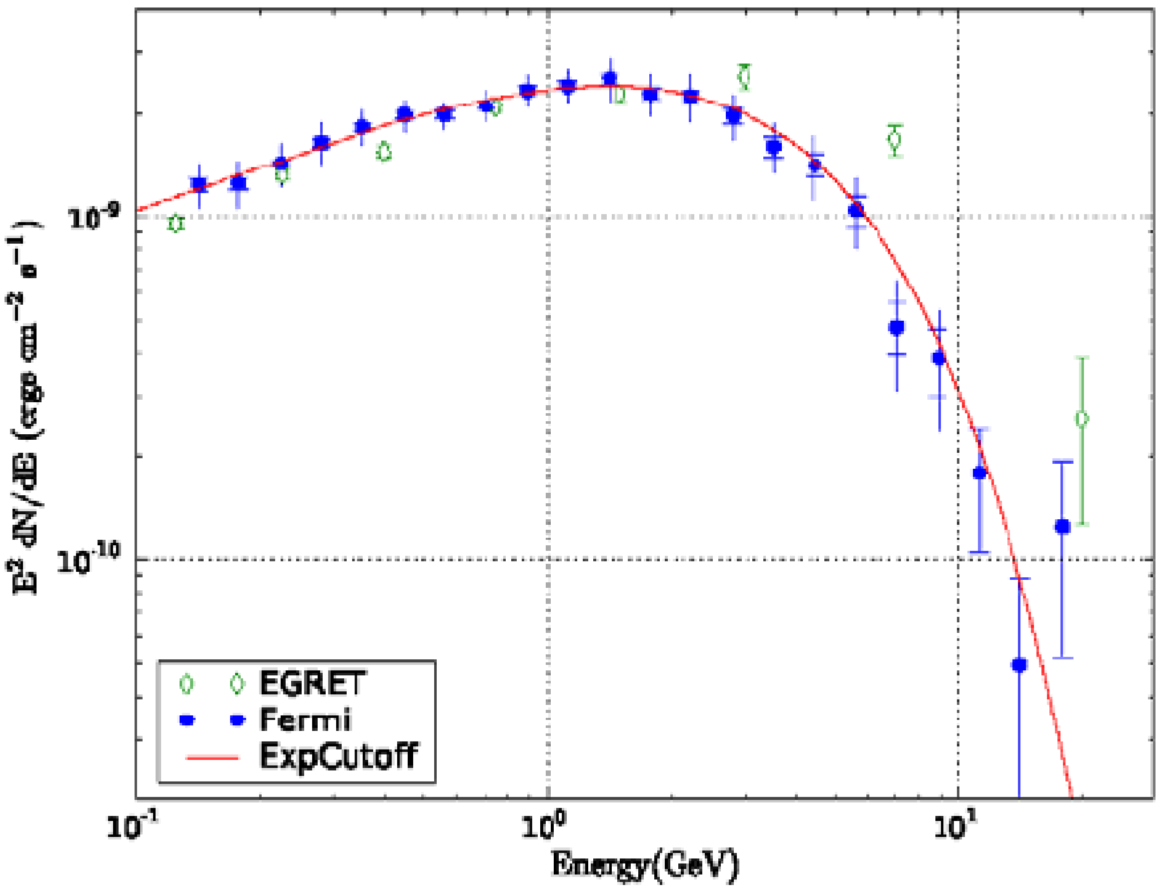

Consistent with b=1 (simple exponential)

$$\Gamma = -1.51^{+0.05}_{-0.04}$$

$$E_c = 2.9 \pm 0.1 \text{ GeV}$$

b=2 (super-exponential) rejected at 16.5σ

No evidence for magnetic pair attenuation: Near-surface emission ruled out

Abdo+09

Caustic でない第3ピーク

Fig. 1 Pulse profile of the Vela pulsar, as a function of energy. The different behavior of the two main peaks is evident. A third peak is seen to appear at higher energies, with its position shifting in phase, as a function of energy (from Abdo et al., 2010k, reproduced by permission of the AAS).

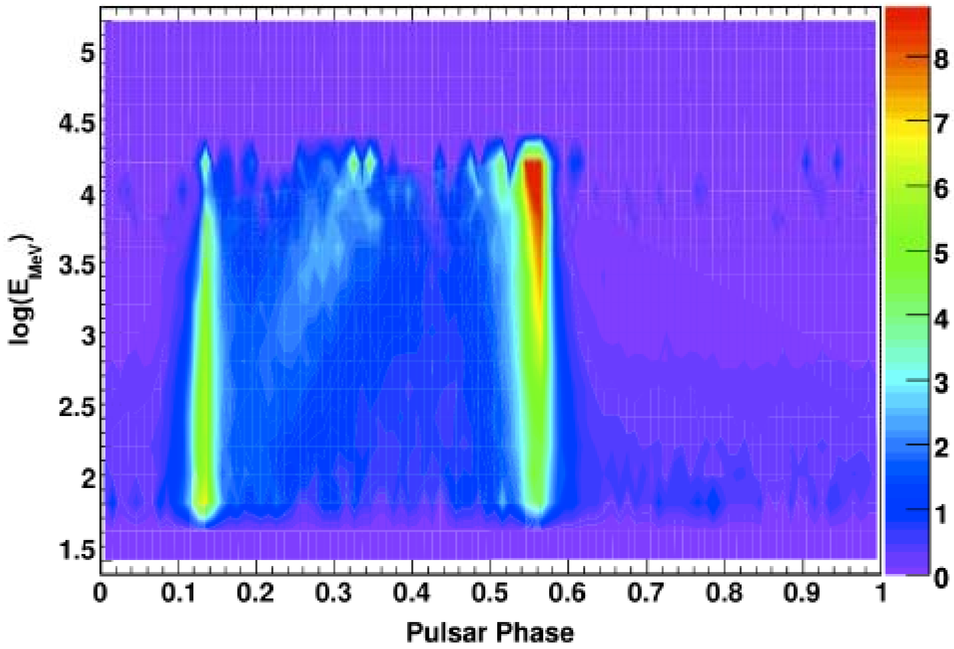

After Ray & Parkinson 2010
Astro-ph 1007.2183

Radio

Vela Pulsar

ガンマ線

(Harding et al. 2002)

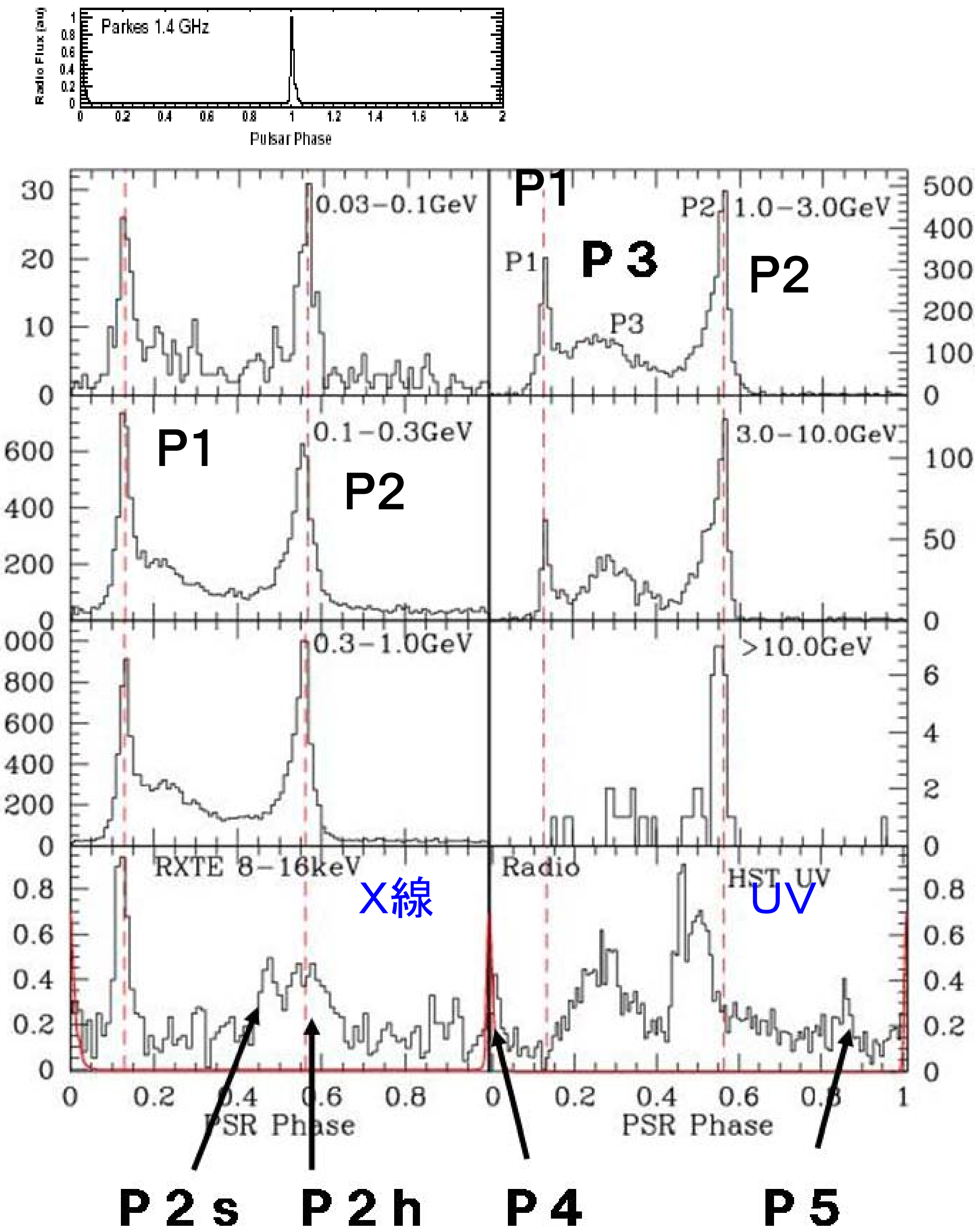

Ec が高いP3

$dE = K\, E^{-\Gamma} \exp(-E/Ec)\, dE$

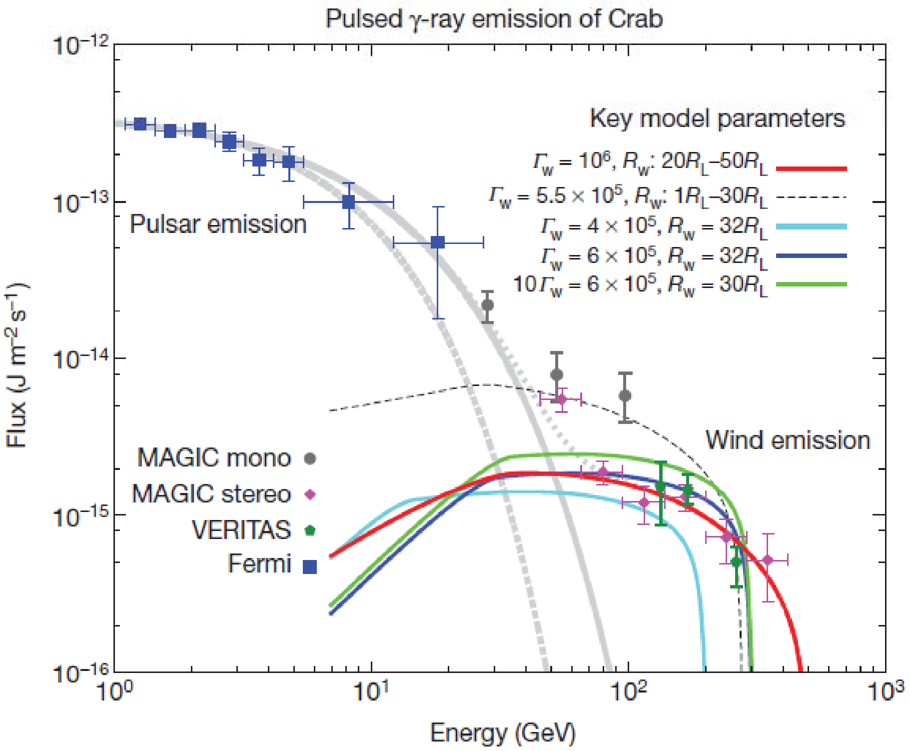

Aharonian & Bogovalov 2012 nat 482 507

さらに高エネルギーの
パルス成分 (Crab)

MAGIC 100MeV
Klepser et al. 2012

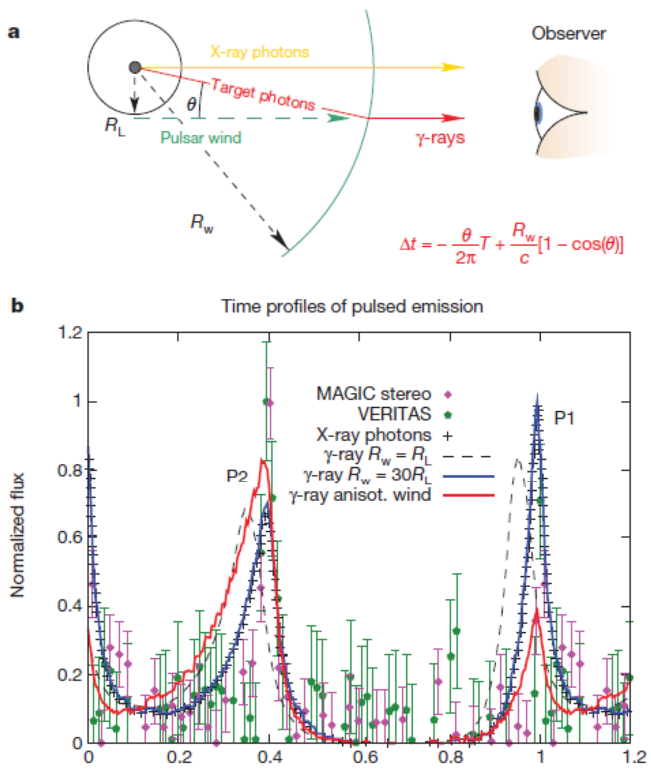

(20-50)R_LC で"wind"加速 EM➔KE

nGJ × RLC × σT = 10^-7

Windが早々に high sigma ➔ low sigma ? と単純に考えないでください。
もともとちぎれるところは high sigma でない、reconnection もあり、
構造を考えないといけない。Multiplicity n/nGJも気になる。

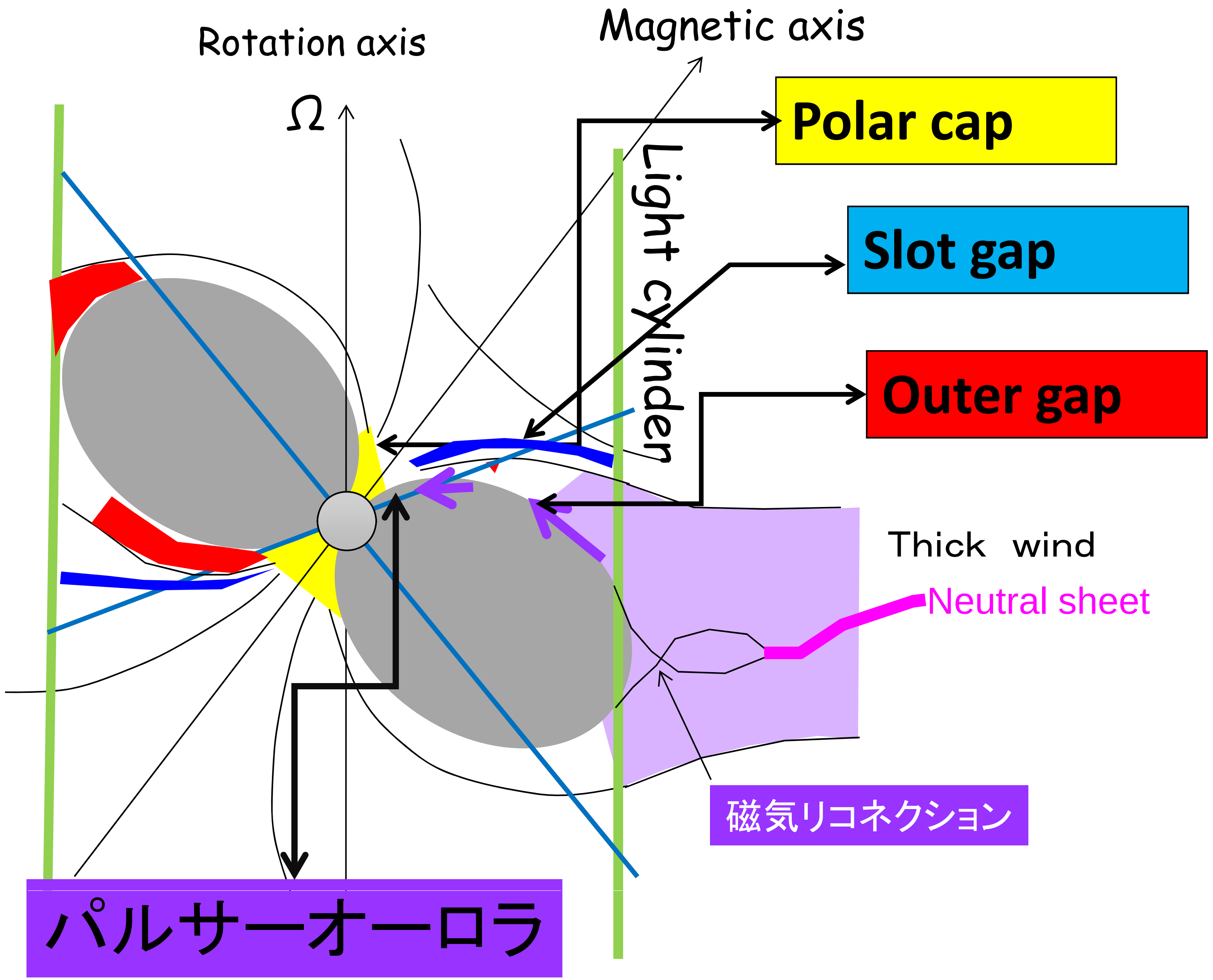

Rotation axis
Magnetic axis
Ω
Polar cap
Slot gap
Outer gap
Light cylinder
Thick wind
Neutral sheet
磁気リコネクション
パルサーオーロラ

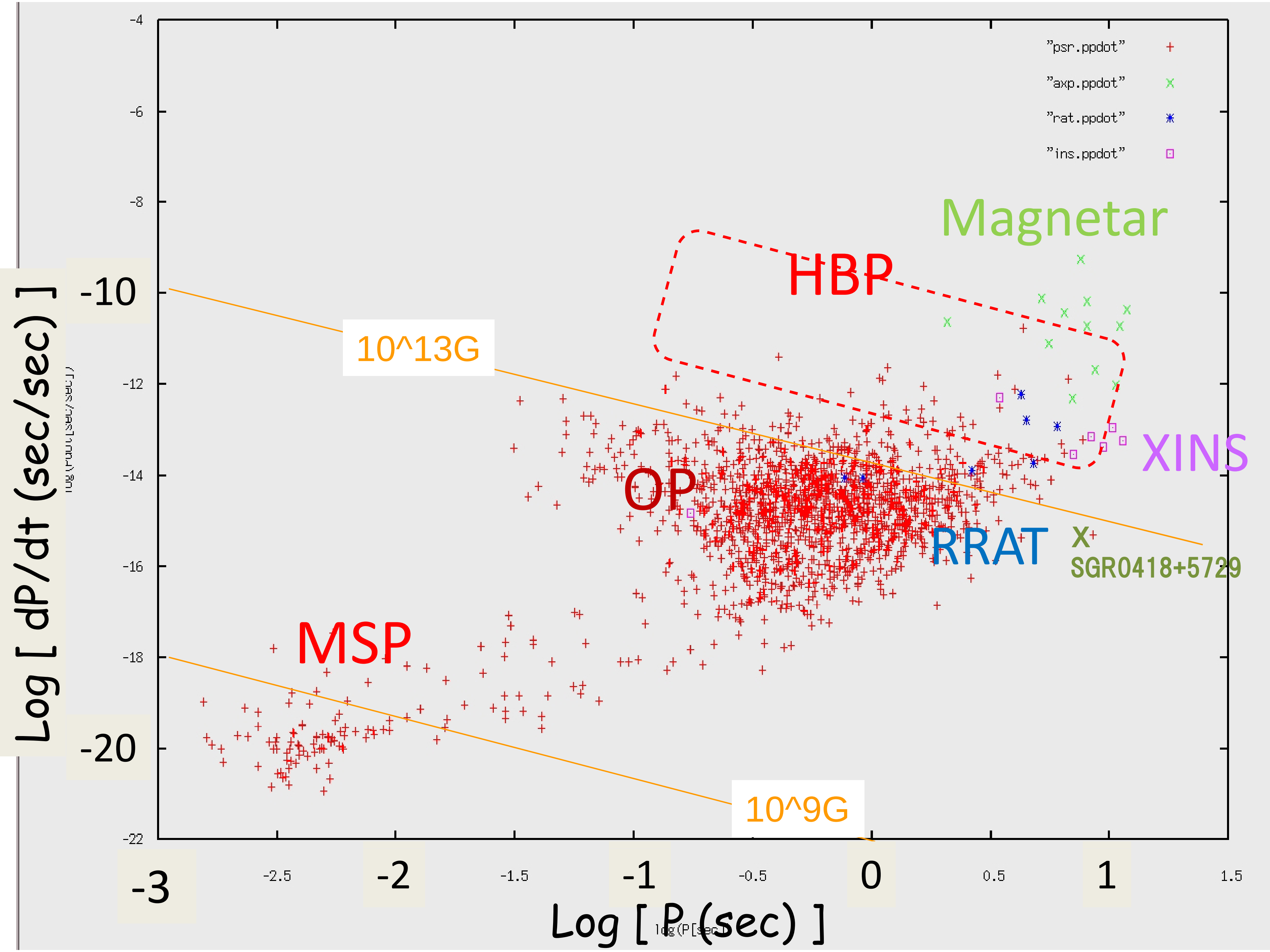

"psr.ppdot"
"axp.ppdot"
"rat.ppdot"
"ins.ppdot"
Magnetar
HBP
10^13G
OP
XINS
RRAT
SGR0418+5729
MSP
10^9G
Log [dP/dt (sec/sec)]
Log [P (sec)]
-4
-6
-8
-10
-12
-14
-16
-18
-20
-22
-3
-2.5
-2
-1.5
-1
-0.5
0
0.5
1
1.5

マグネターとパルサーの違いを説明する作業仮説

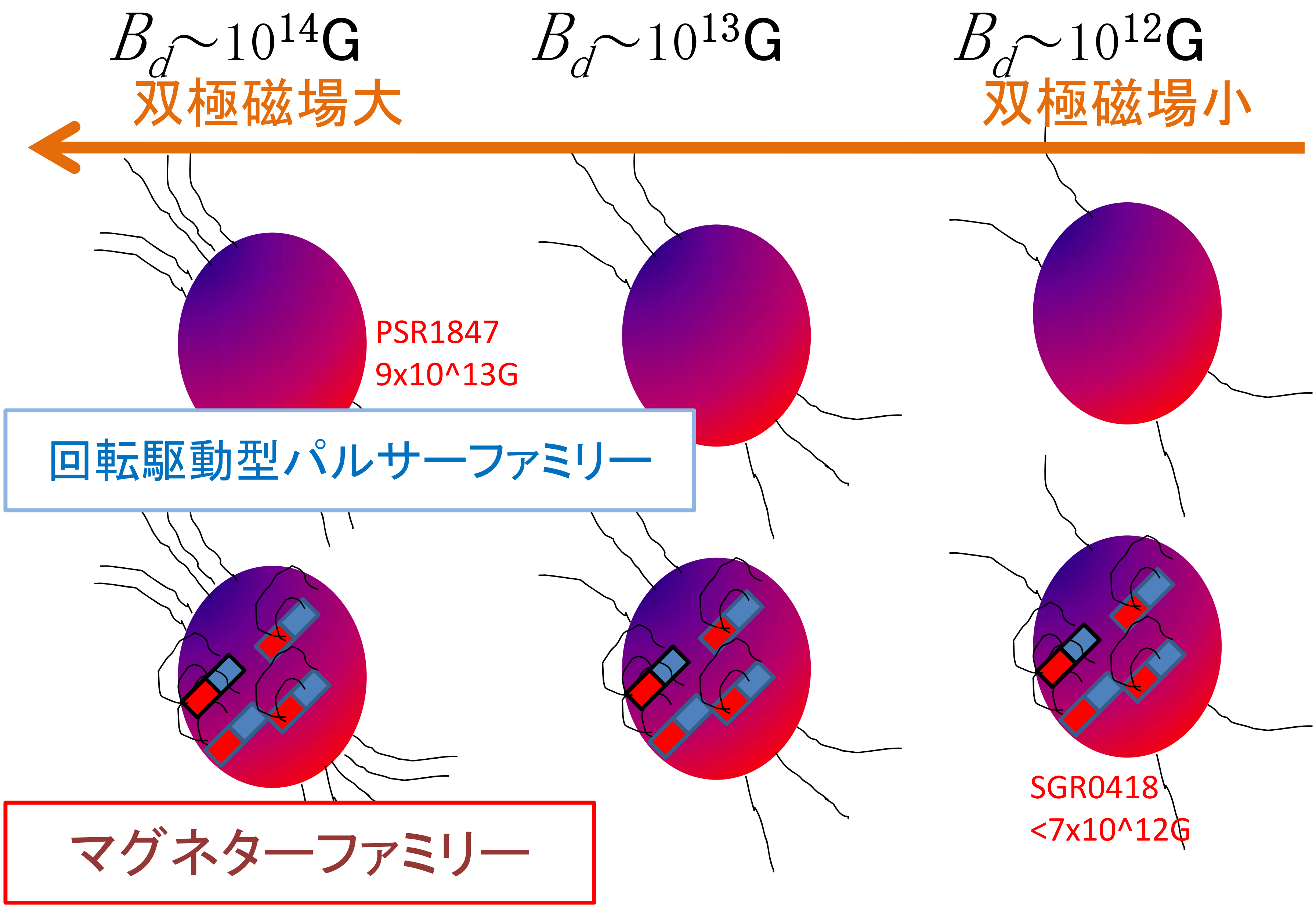

How do we discriminate RPP and magnetar?

Lx(0.1-2keV) Becker, W., 2009, Astrophysics and Space Science Library, 357, 91
empirical law: Lx = Lrot 10^-3 +/- 1

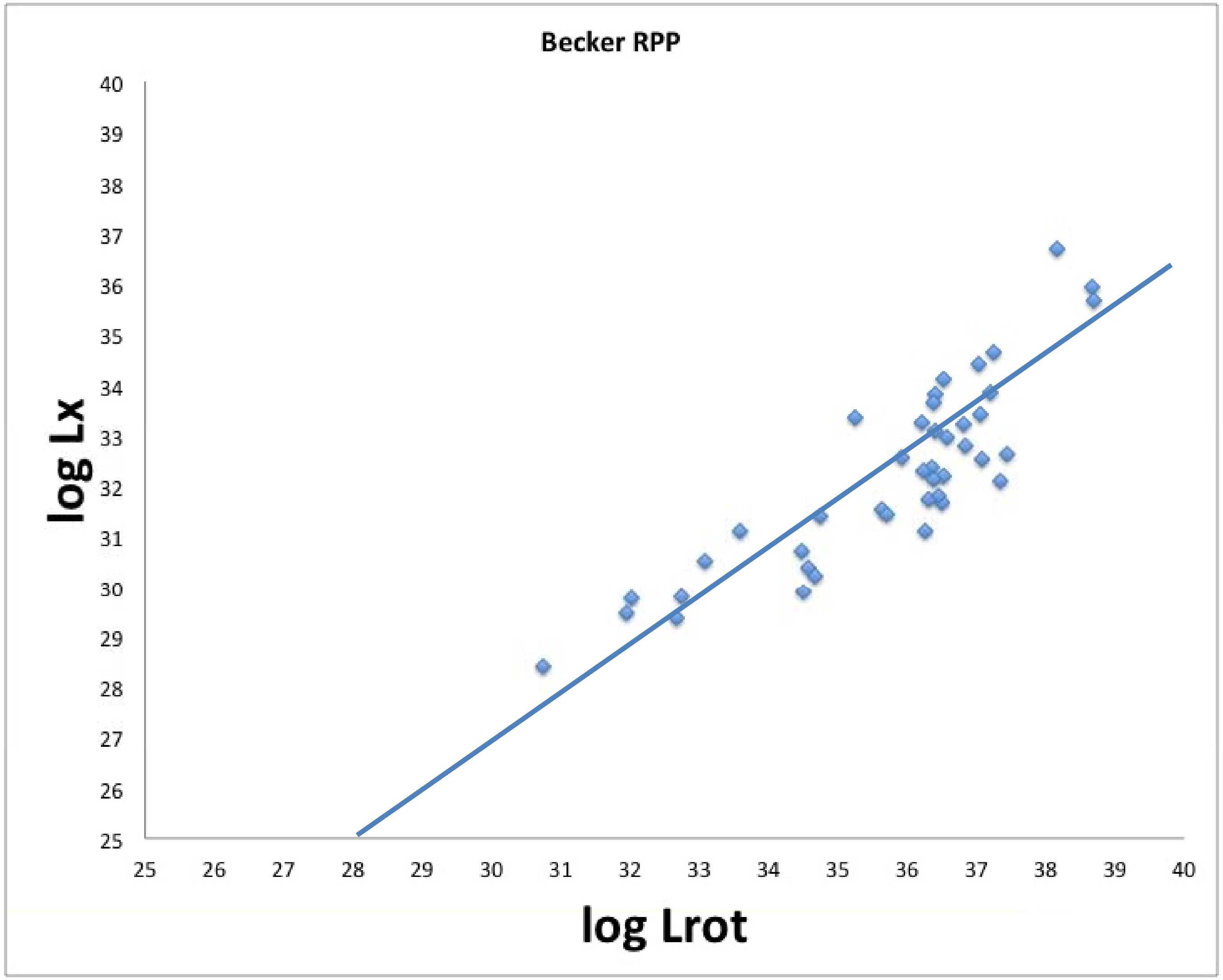

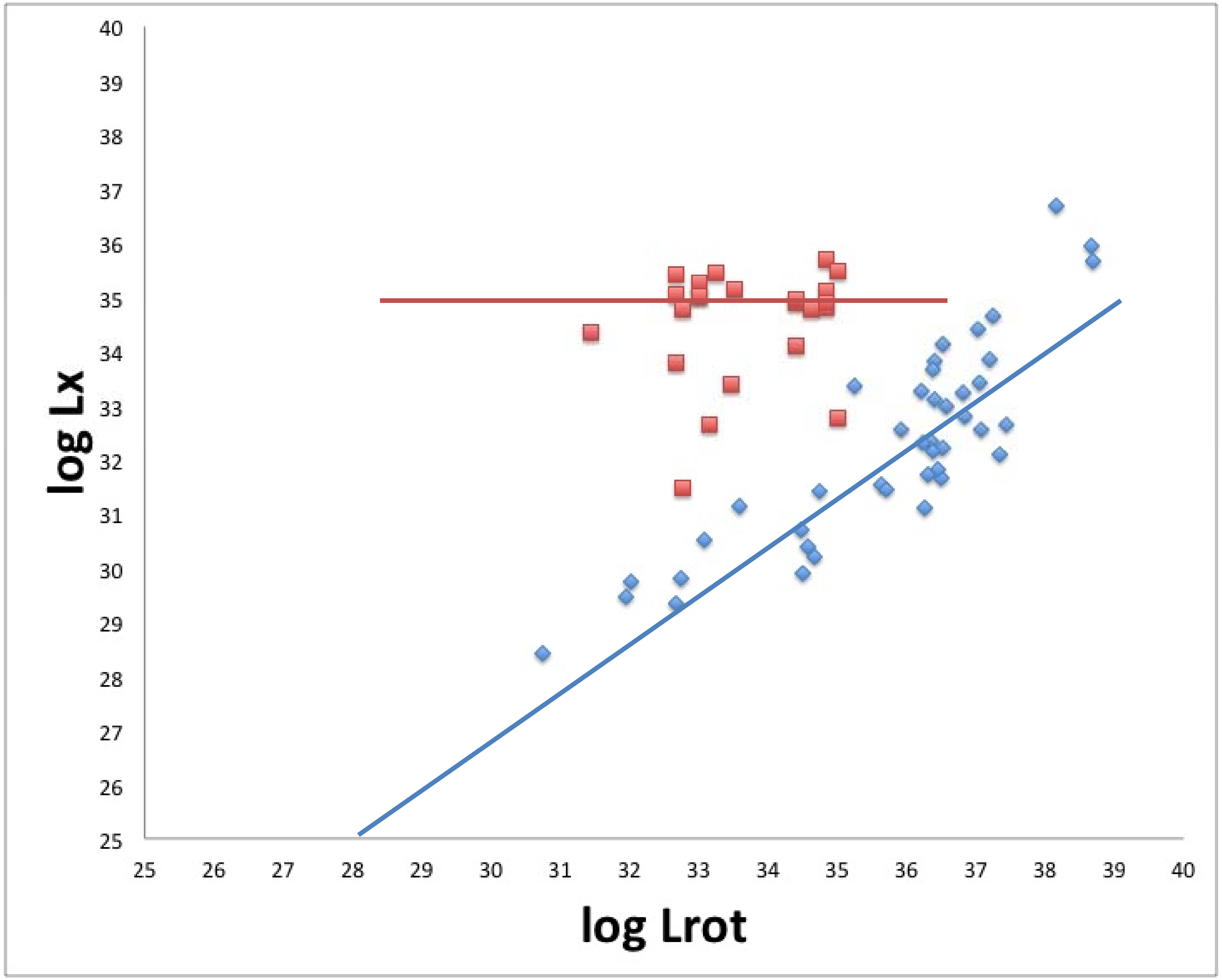

log Lx
log Lrot
40
39
38
37
36
35
34
33
32
31
30
29
28
27
26
25
25
26
27
28
29
30
31
32
33
34
35
36
37
38
39
40

J1808-2024	7.556	15.314	13.100	AXP,NRAD
J1841-0456	11.779	14.866	7.500	AXP,NRAD
J1048-5937	6.452	14.701	9.000	AXP,NRAD
J1708-4009	11.001	14.669	3.800	AXP,NRAD
J0100-7211	8.020	14.594	60.600	AXP,NRAD
J1622-4950	4.326	14.438	9.140	PSR*Mactive$¥eta=$0.31
J1550-5418	2.070	14.346	9.740	AXP,HE
J1809-1943	5.540	14.322	3.570	AXP,HE
J0146+6145	8.689	14.127	3.600	AXP,NRAD
J1847-0130	6.707	13.971	7.640	PSR,no_constraint$¥eta<$25
J1718-3718	3.379	13.873	6.060	PSR,Mactive¥eta=$0.12
J2301+5852	6.979	13.769	3.200	AXP,NRAD
J1814-1744	3.976	13.741	9.770	PSR,no_contraint$¥eta<$12
J1734-3333	1.169	13.718	7.400	PSR,HE[oklk10],normal$¥eta=$0.0012
J1819-1458	4.263	13.700	3.810	RRAT,HE,Mactive$¥eta=$15.3
J1846-0258	0.327	13.688	5.100	NRAD,Mactive/normai?$¥eta=$0.002
J1119-6127	0.408	13.613	8.400	HE[gkc+07]
J1821-1419	1.656	13.590	11.930	*
J1746-2850	1.077	13.585	12.860	*
J1726-3530	1.110	13.571	9.970	*
J0726-2612	3.442	13.507	3.010	*
J0534-6703	1.818	13.449	48.100	*
J1846-0257	4.477	13.433	4.690	RRAT
J0847-4316	5.977	13.433	13.440	RRAT
J1854+0306	4.558	13.415	4.110	RRAT
J0720-3125	8.391	13.389	0.360	XINS,NRAD
J1632-4818	0.813	13.367	8.540	*
J1001-5939	7.734	13.338	3.300	*
J1913+0446	1.616	13.332	3.410	*
B0154+61	2.352	13.328	1.610	*
J1524-5706	1.116	13.305	21.590	*

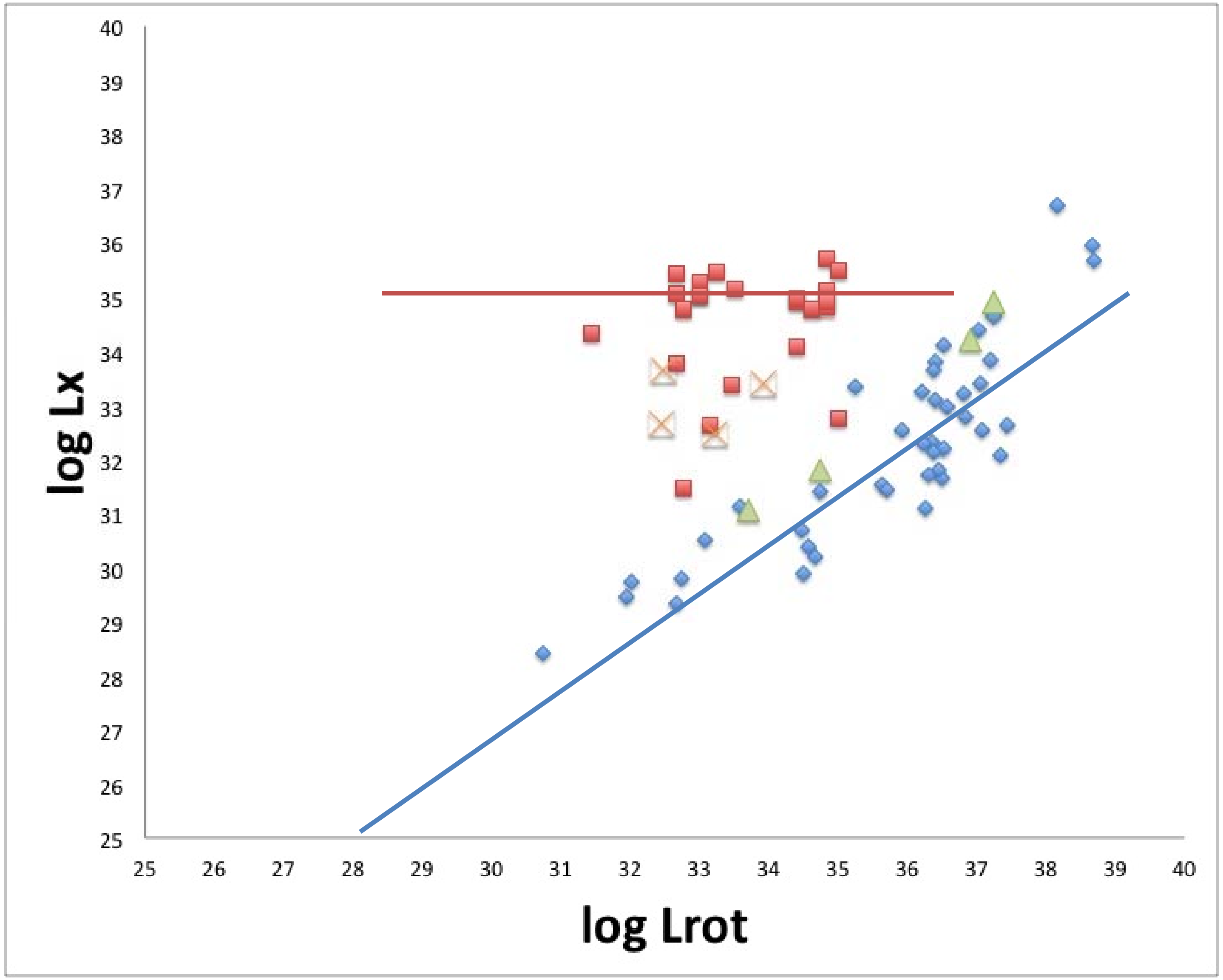

log Lx
40
39
38
37
36
35
34
33
32
31
30
29
28
27
26
25
25
26
27
28
29
30
31
32
33
34
35
36
37
38
39
40
log Lrot

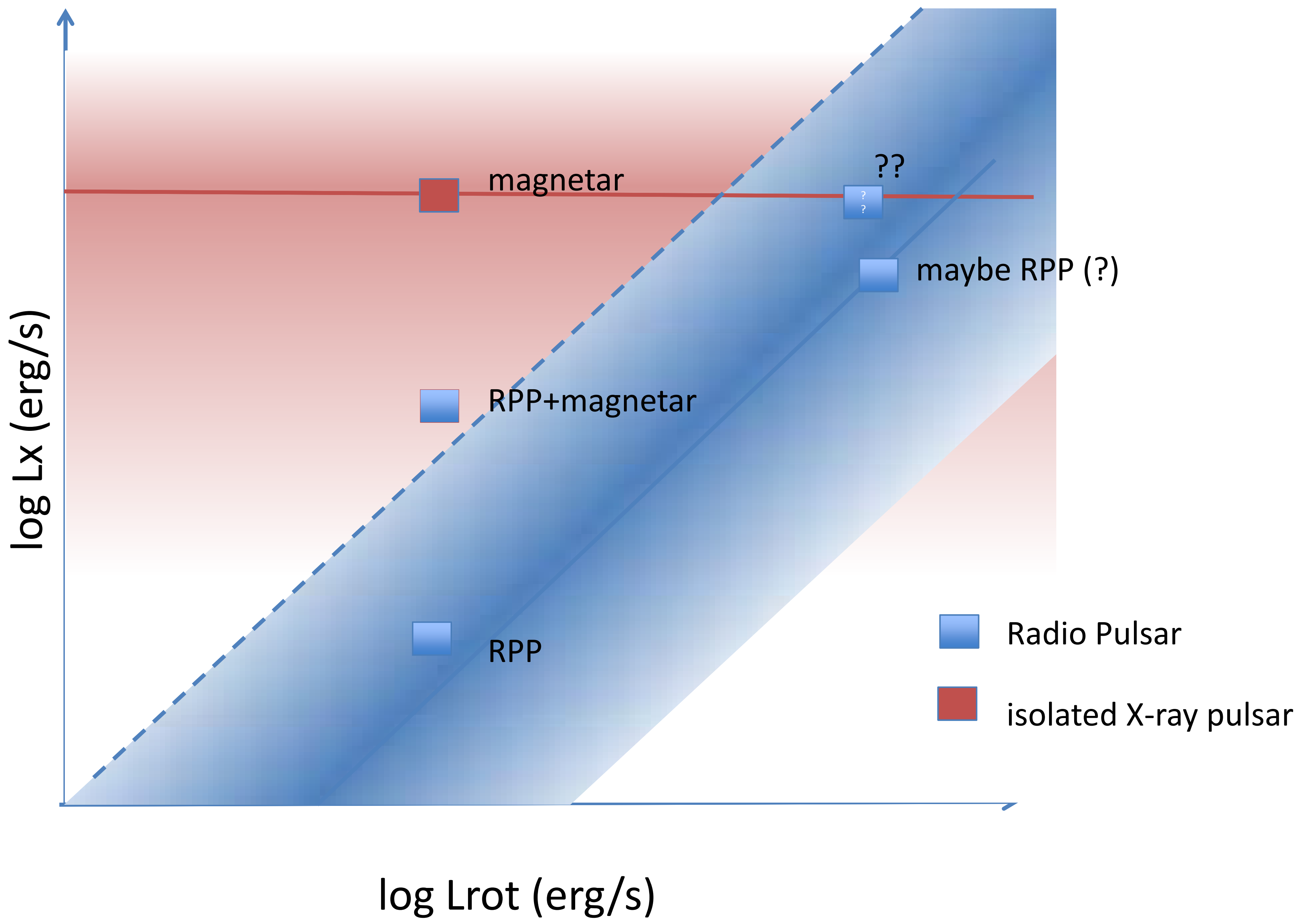

log Lx (erg/s)
magnetar
??
?
?
maybe RPP (?)
RPP+magnetar
RPP
Radio Pulsar
isolated X-ray pulsar
log Lrot (erg/s)

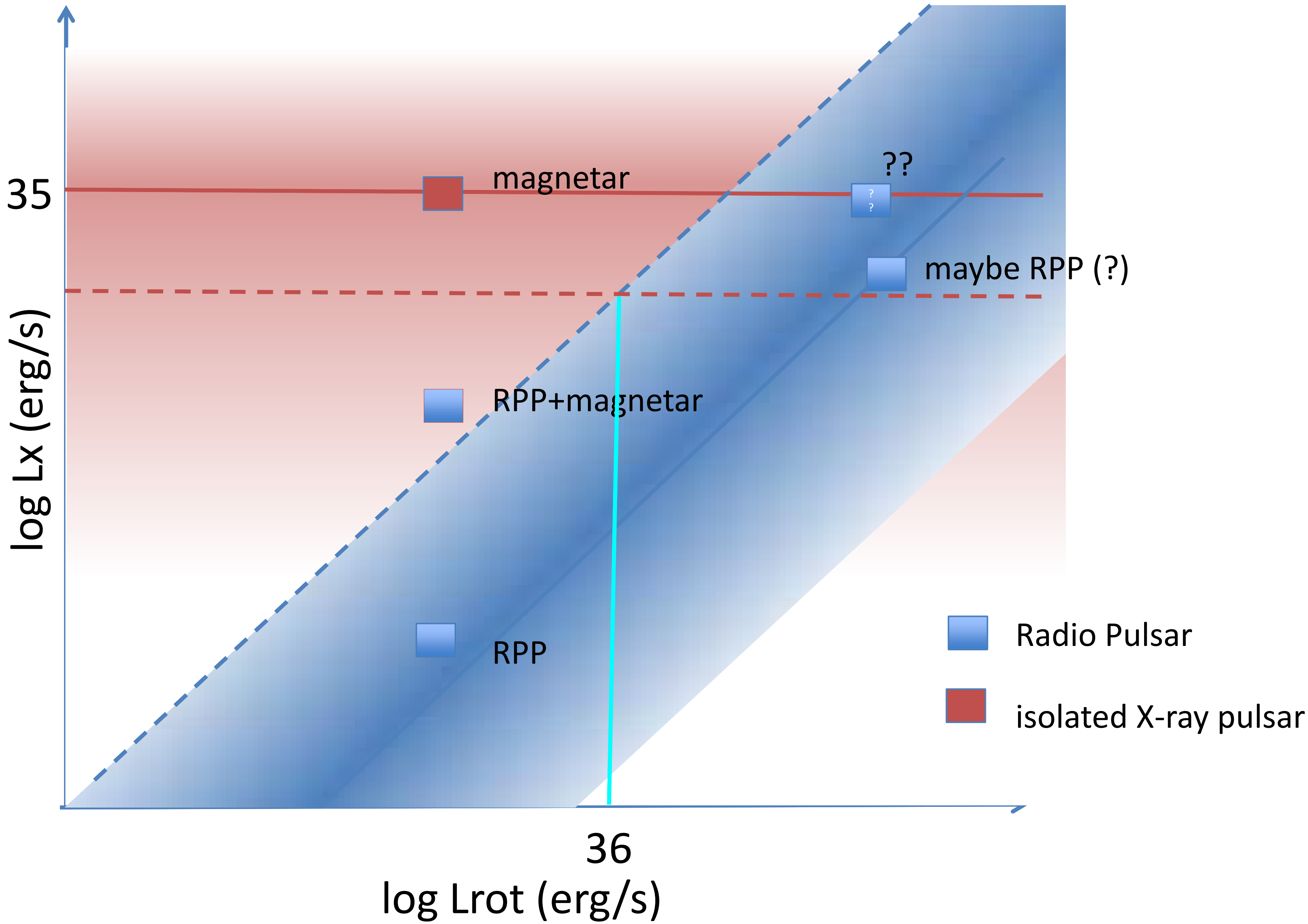

35
log Lx (erg/s)
magnetar
??
maybe RPP (?)
RPP+magnetar
RPP
36
log Lrot (erg/s)
Radio Pulsar
isolated X-ray pulsar

Pick up all the Radio Pulsars (RPP) from Perkes catalog

1759 entries

if (Lrot/4πD^2) × (1/100) > (limiting flux to identify the object)

& Lrot < 10^36 erg/sec,

then

detected ➔ can be diagnosed if magnetar like radio pulsar or normal RPP

not detected ➔ normal RPP

eg, for F_lim = 10^-12.5 erg/cm^2 sec, 107 entries

THE ASTROPHYSICAL JOURNAL SUPPLEMENT SERIES, 134:77–102, 2001 May
© 2001. The American Astronomical Society.. All rights reserved. Printed in U.S.A.

FAINT X-RAY SOURCES RESOLVED IN THE *ASCA* GALACTIC PLANE SURVEY AND THEIR CONTRIBUTION TO THE GALACTIC RIDGE X-RAY EMISSION

MUTSUMI SUGIZAKI[1]
Tsukuba Space Center, National Space Development Agency of Japan, 2-1-1 Sengen, Tsukuba, Ibaraki 305-8505, Japan; sugizaki@oasis.tksc.nasda.go.jp
KAZUHISA MITSUDA, HIDEHIRO KANEDA, AND KEIICHI MATSUZAKI
Institute of Space and Astronautical Science, 3-1-1 Yoshinodai, Sagamihara, Kanagawa 229-8510, Japan
SHIGEO YAMAUCHI
Faculty of Humanities and Social Sciences, Iwate University, 3-18-34 Ueda, Morioka, Iwate 020-8550, Japan
AND

PSR B1830-08
(Lx/Lrot=0.0028)

163 point soucrs

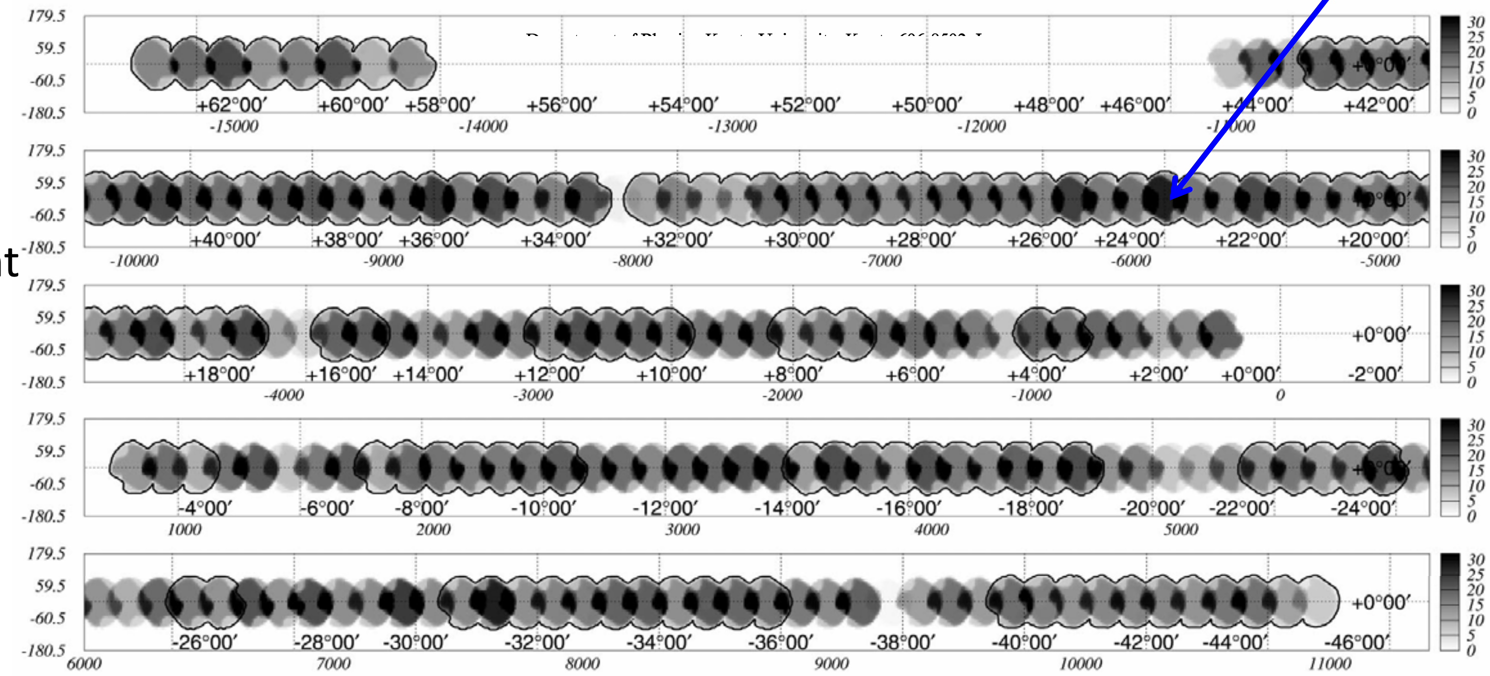

|l |<45 degree, |b|<0.4 degree with F_lim = 10^-12.5

all normal !

11 entries

Muno M. P., et al., 2009, ApJS, 181,110

Chandra Deep survey of the Galactic Center

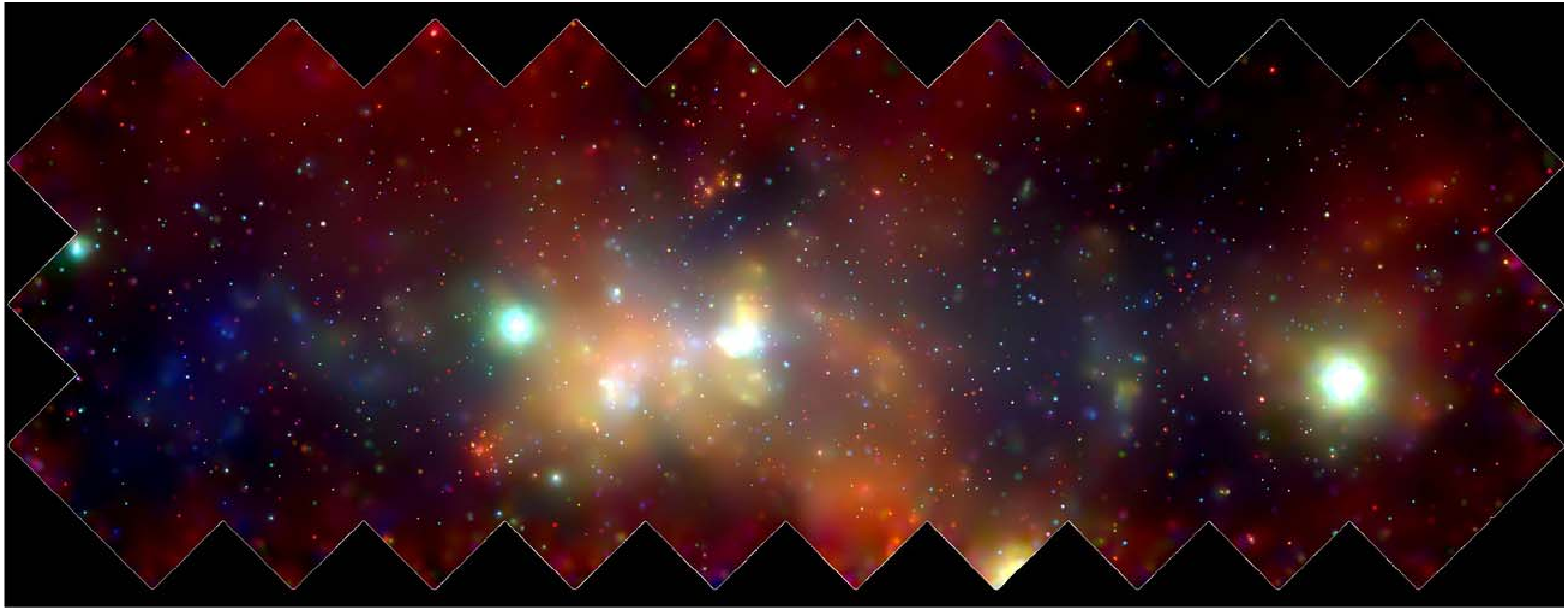

|l |<1 degree, |b|<0.4 degree with F_lim = 10^-16 erg/cm^2 sec

2 entries

all normal !

correction for population

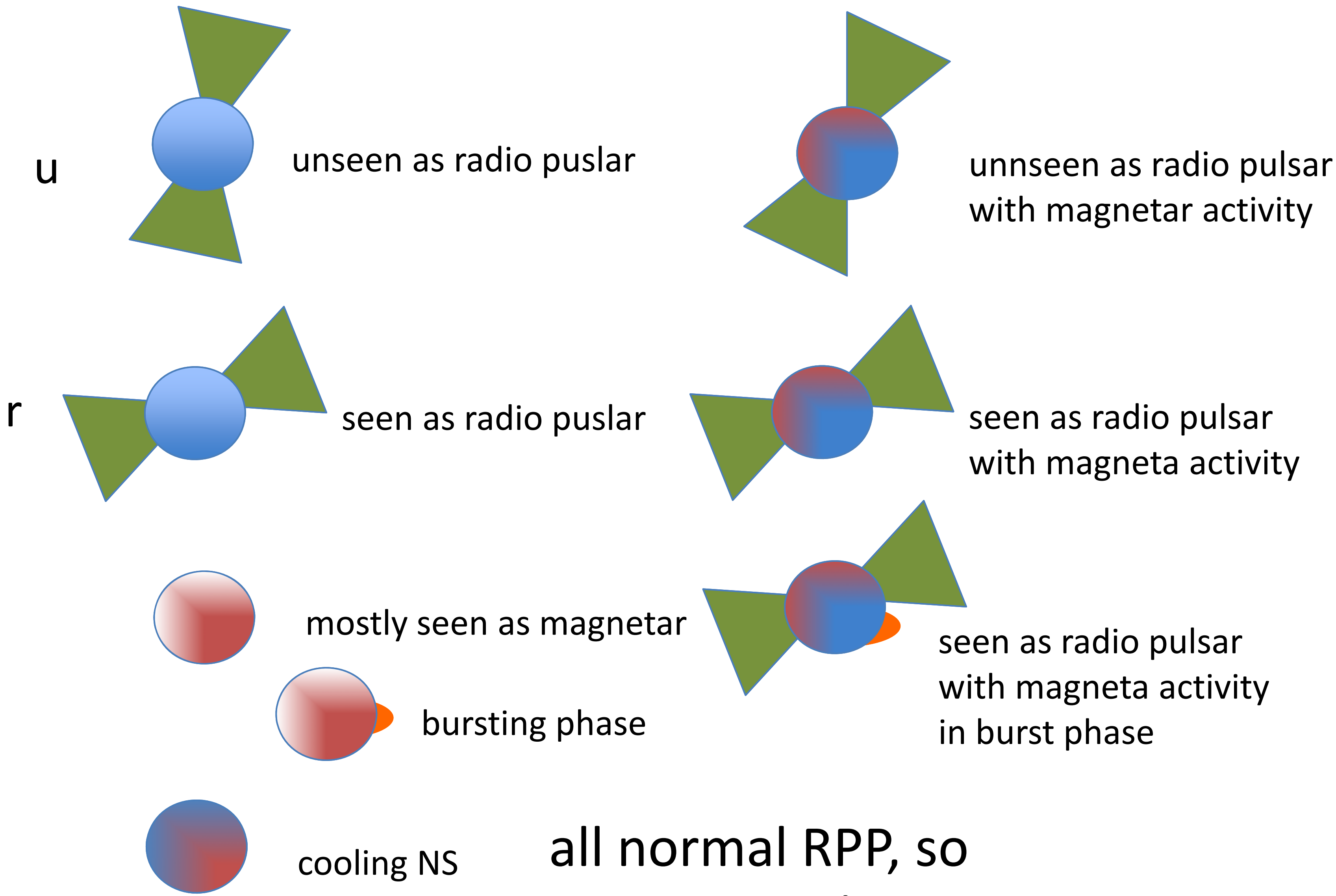

all normal RPP, so

we get $f < 1/13 \times$ (correction factor)

What shall we do to determine f ?

1. Re-analyze ASCA gal. survey, targeted soft-source? F_lim ? 10^-13.5
2. Any other public data?

   181 entries

3. Observe nearby Radio pulsars with what ? (XMM, Chandra Suzaku?)

   42 entries

   Flim = 10^-13.0
   d < 1.0 kpc

PSR J1846-0258 in Kes 75

A Switching Guy between RPP and Magnetar?

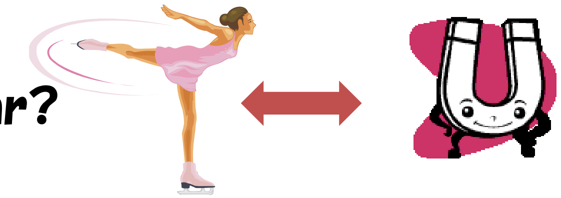

Basic Data:
P = 0.325684, Pdot 7.08E-12, breaking index 2.65
Bd =4.86E+13, age 7.28E+02, log(Lrot [erg/sec])= 36.907949
Distance= 5.1kpc in Perkes cat. (can be 10.6 kpc, 5.1-21 kpc not certain)

Note:
X-ray selected pulsar (RXTE+ASCA), NO radio pulses, High B,
in SNR Kes 75, normal PWN (Chandra, HESS)
In 7-12 June 2006 , a magnetar-like outburst,
increase of Fx and glitch took place

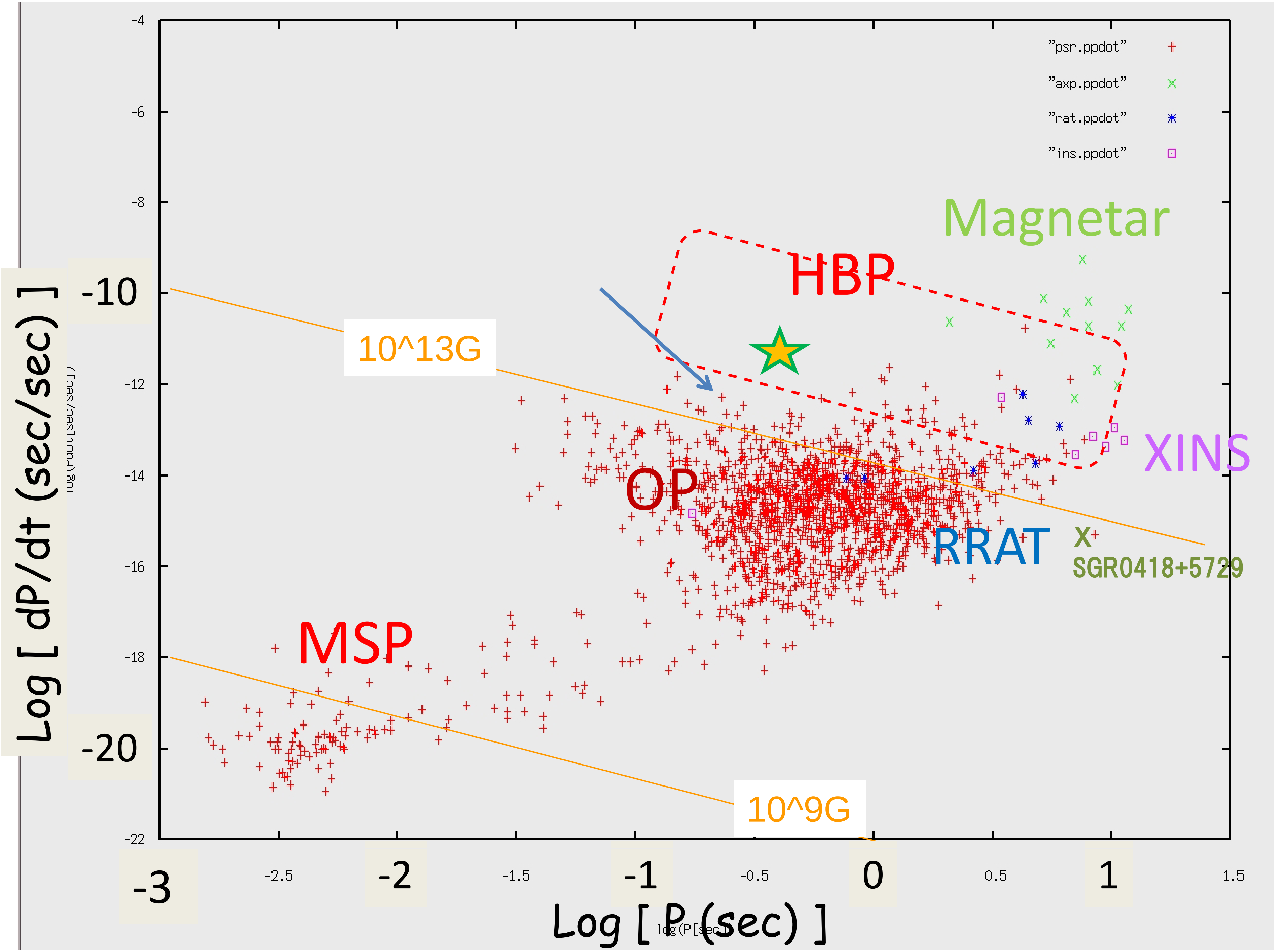

"psr.ppdot"
"axp.ppdot"
"rat.ppdot"
"ins.ppdot"
Magnetar
HBP
XINS
OP
RRAT
SGR0418+5729
MSP
10^13G
10^9G
Log [dP/dt (sec/sec)]
Log [P (sec)]
-4
-6
-8
-10
-12
-14
-16
-18
-20
-22
-3
-2.5
-2
-1.5
-1
-0.5
0
0.5
1
1.5

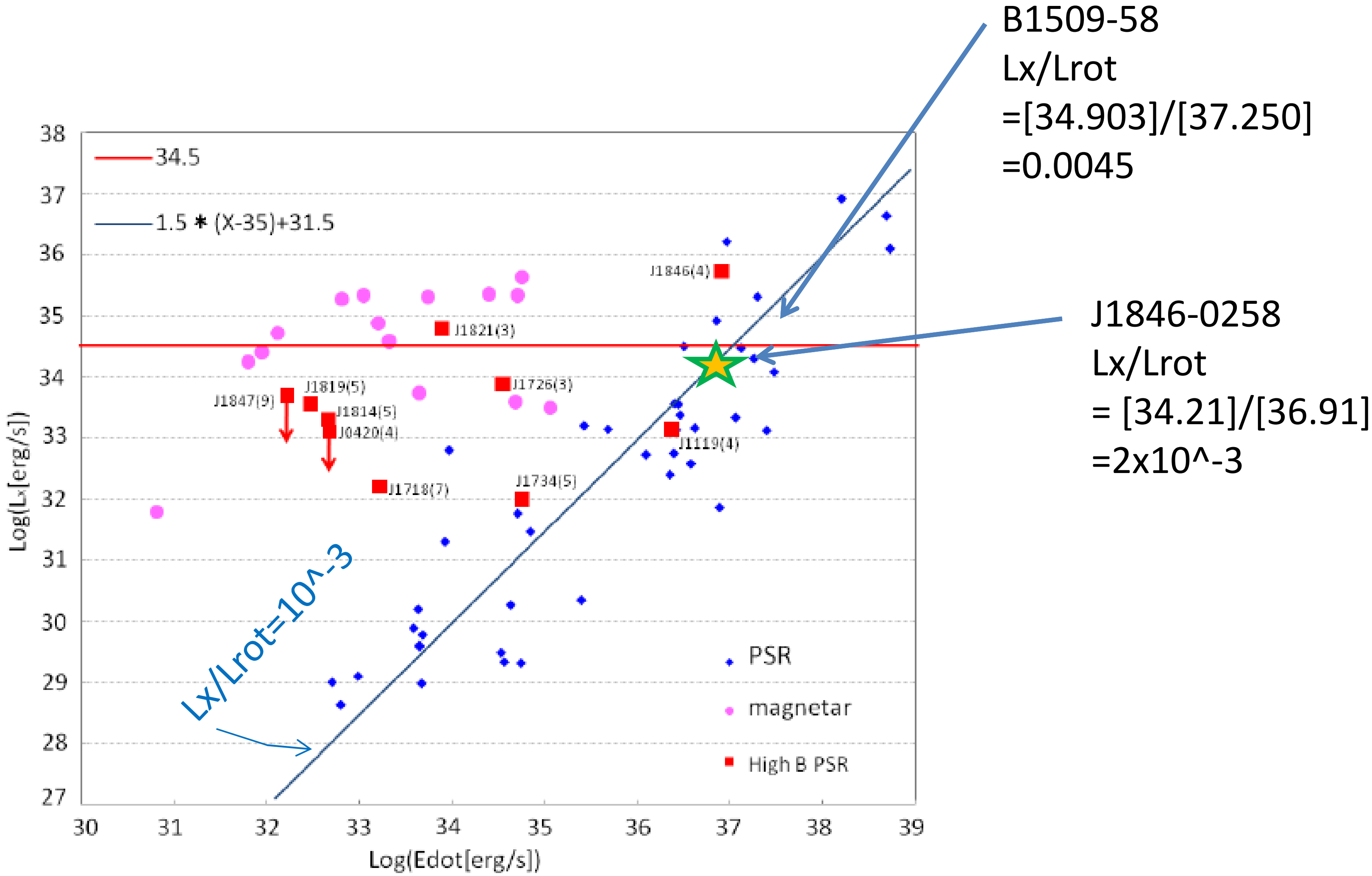

図 1: 回転駆動型パルサーとマグネターに対する回転パワー-対 X 線光度図

J1846-0258

L. Kuiper and W. Hermsen: High-energy characteristics of the schizophrenic pulsar PSR J1846−0258 in Kes 75

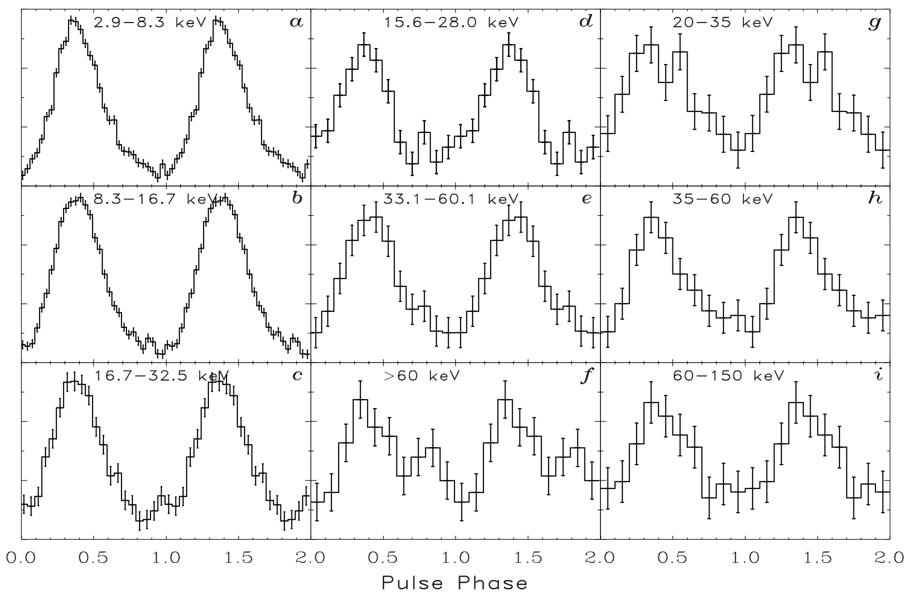

B 1509-58

G. Cusumano et al.: The curved X-ray spectrum of PSR B1509−58 observed with BeppoSAX

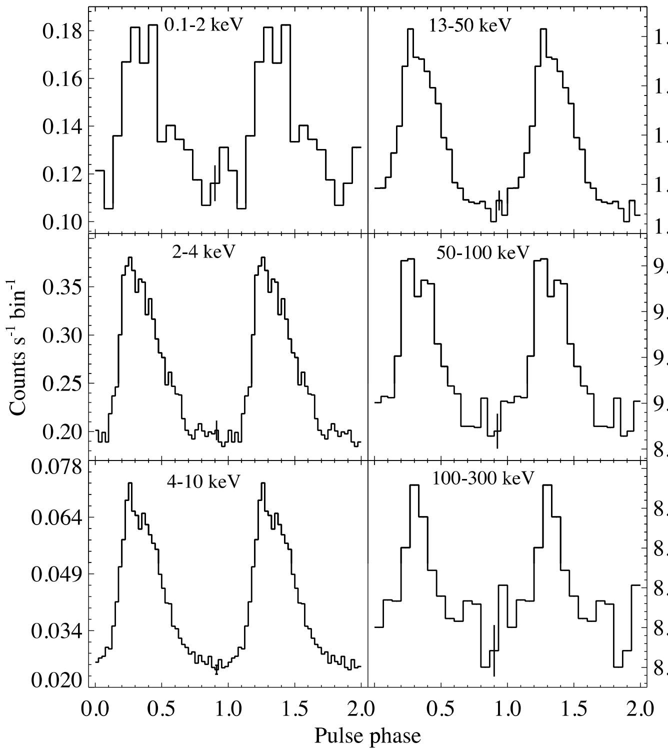

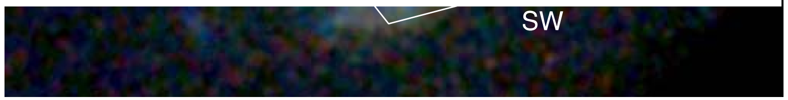

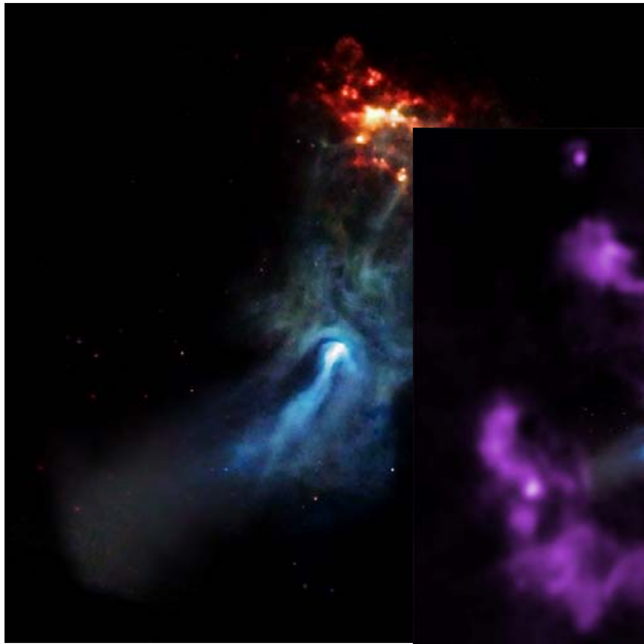

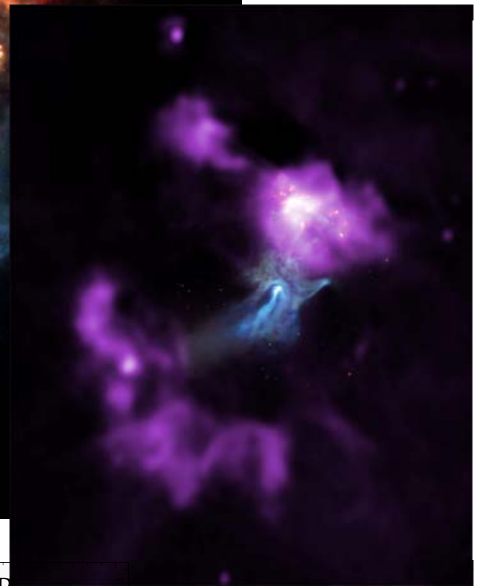

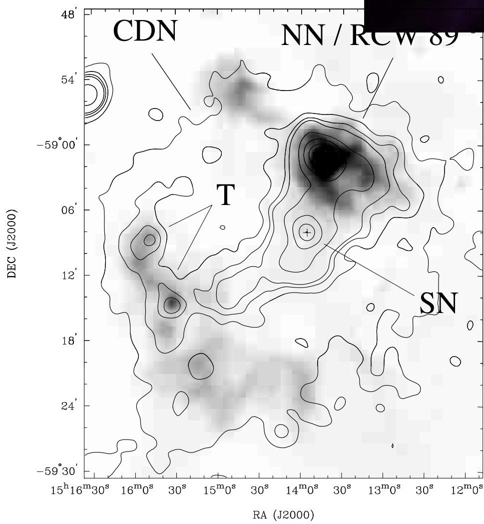

Fig. 1. Radio image of MSH 15–52 (36 cm) with the contour plot from the ROSAT PSPC observation (0.1–2.4 keV). The cross marks the position of PSR B1509–58 (Gaensler et al. 1999). NN and SN indicate the Northern and Southern Nebulae respectively, T is the tail component and CDN the Central Diffuse Nebula.

Mineo, T., Cusumano, G., Maccarone, M.~C., et al.¥ 2001, ¥aap, 380, 695

Before, After and during the out burst; What is different?

No pulse profile change

Flux increase during burst; yes by definition

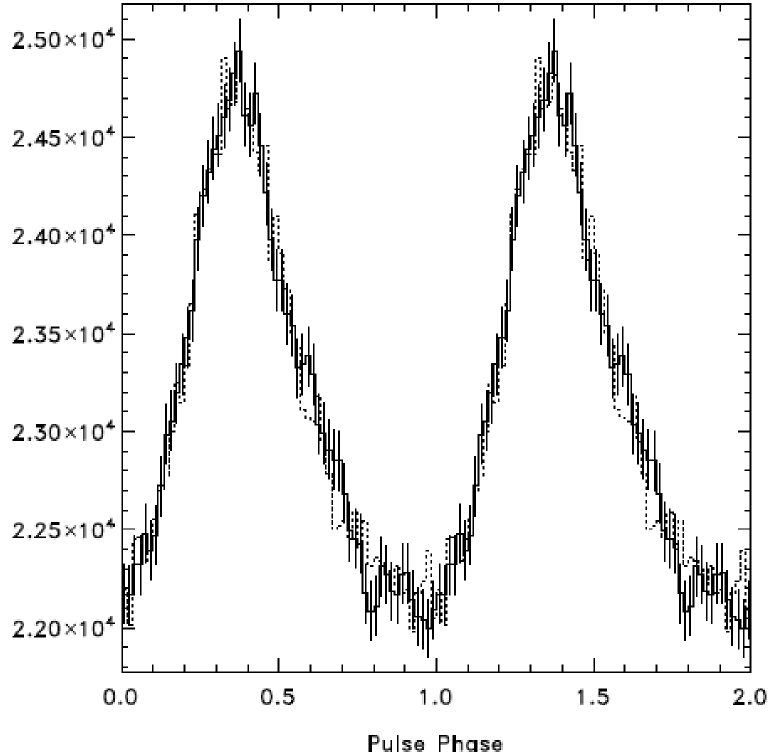

Fig. 5. Comparison of the pulse-profiles accumulated in the PCA PHA band 7–19 (~2.9–8.3 keV) during the early phase of the outburst (Outburst A1+A2, see Table 3, solid histogram with 1σ error bars) and from the pre-outburst observations (high-statistics dotted histogram). No significant shape change is observed, see text. The Y-axis specifies the number of counts per bin.

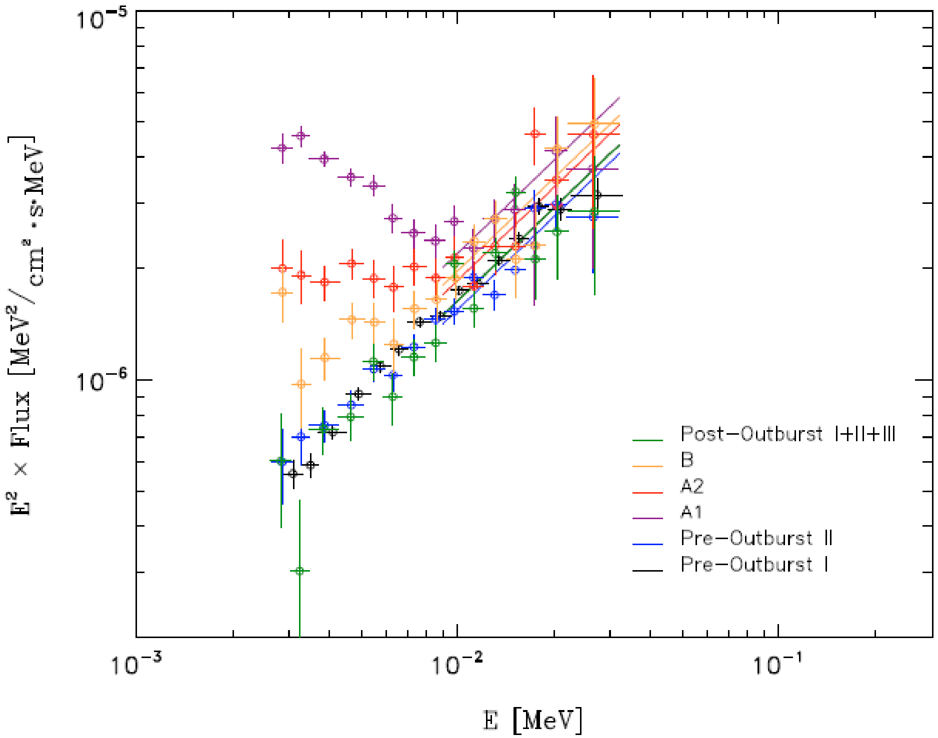

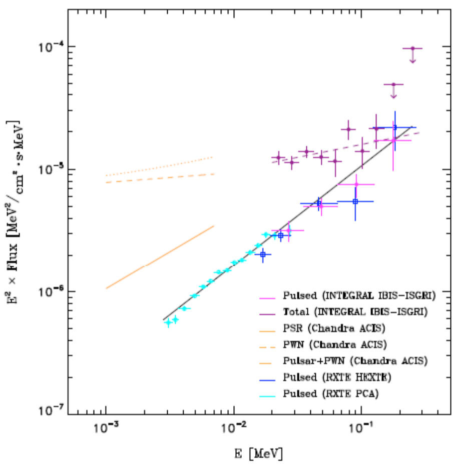
E^2 × Flux [MeV^2/cm^2 · s · MeV]
E [MeV]
Pulsed (INTEGRAL IBIS–ISGRI)
Total (INTEGRAL IBIS–ISGRI)
PSR (Chandra ACIS)
PWN (Chandra ACIS)
Pulsar+PWN (Chandra ACIS)
Pulsed (RXTE HEXTE)
Pulsed (RXTE PCA)

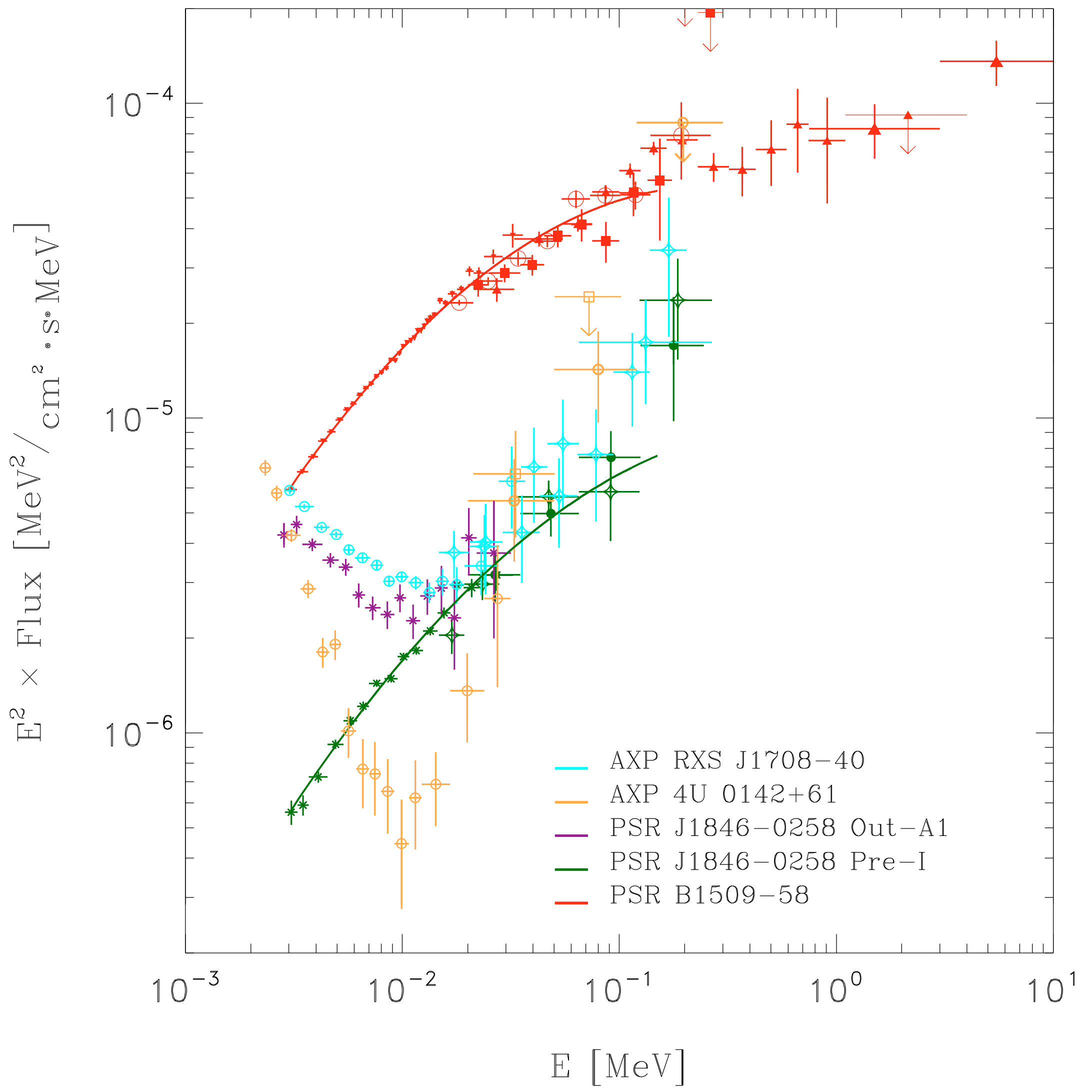
E^2 × Flux [MeV^2/cm^2 · s · MeV]
E [MeV]
AXP RXS J1708−40
AXP 4U 0142+61
PSR J1846−0258 Out−A1
PSR J1846−0258 Pre−I
PSR B1509−58

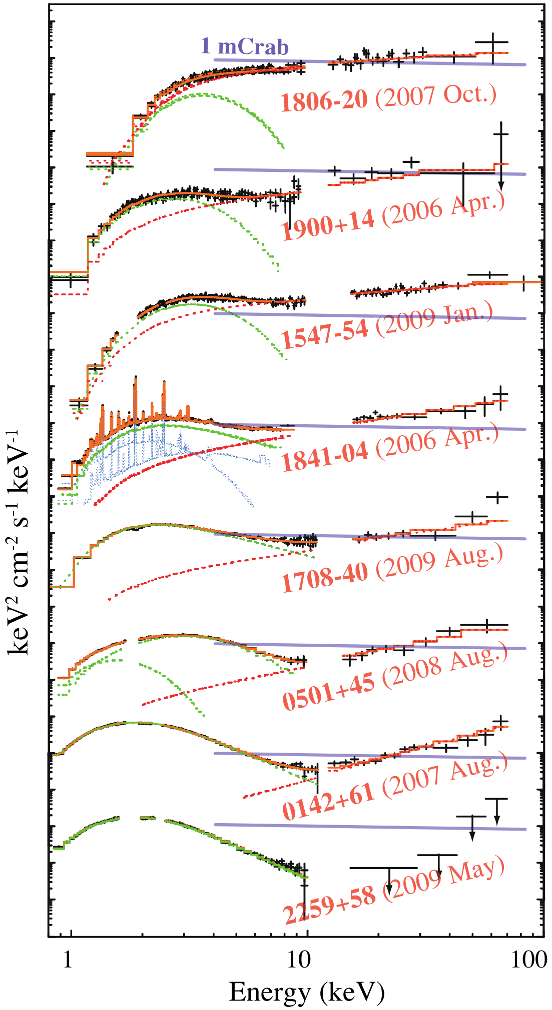
1 mCrab
1806-20 (2007 Oct.)
1900+14 (2006 Apr.)
1547-54 (2009 Jan.)
1841-04 (2006 Apr.)
1708-40 (2009 Aug.)
0501+45 (2008 Aug.)
0142+61 (2007 Aug.)
2259+58 (2009 May)
keV² cm⁻² s⁻¹ keV⁻¹
1
10
100
Energy (keV)

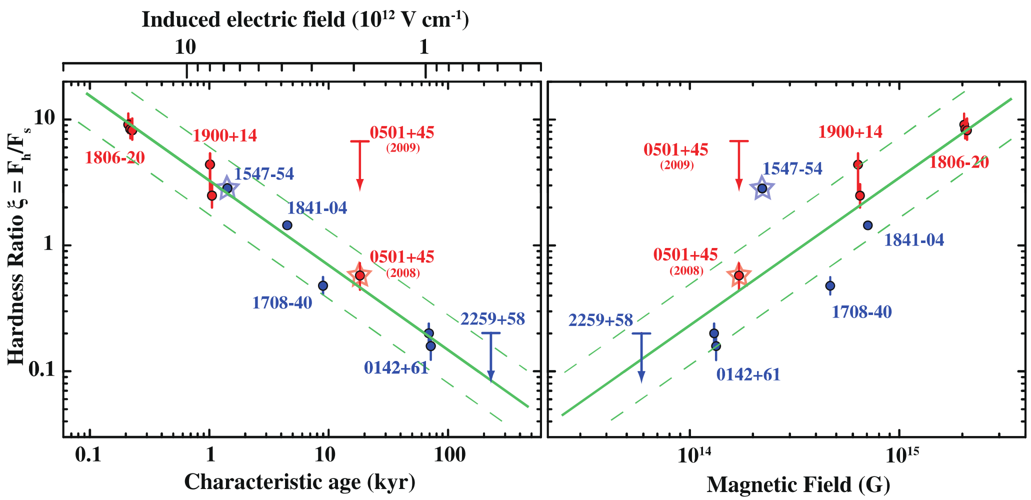
Induced electric field (10¹² V cm⁻¹)
10
1
Hardness Ratio ξ = F_h/F_s
10
1
0.1
1806-20
1900+14
0501+45 (2009)
1547-54
1841-04
0501+45 (2008)
1708-40
2259+58
0142+61
0.1
1
10
100
Characteristic age (kyr)
10¹⁴
10¹⁵
Magnetic Field (G)

How different the magnetospheric process?

normal RPP

emf+pair creation, PW, outer gap, pulsar wind (PWN)

normail RPP with magnetic activity (eg. heating, non-thermal rad. burst,,)

➔intermediate ??

magnetar

heating+non-thermail rad. short burst + outburst

(radio + outer gap) suppressed

How different magnetic field generation?

NS formation (rotation original field explosion,,,,)

dynam

f = (intermediate)/(RPP)

f(B_d, τ)